electronics

MDPI

Article

Rapid Non-Invasive Capacitive Assessment of Extra Virgin Olive Oil Authenticity

Hari Krishna Salila Vijayalal Mohan *, Pyei Phyo Aung, Chee Fong Ng, Zheng Zheng Wong and Andrew Alexander Malcolm

Intelligent Product Verification (IPV), Advanced Remanufacturing and Technology Centre (ARTC), Agency for Science, Technology and Research (A*STAR), 3 Cleantech Loop, CleanTech Two, Singapore 637143, Singapore

* Correspondence: hari_krishna@artc.a-star.edu.sg

Abstract: Economically motivated adulteration (EMA) and/or cross-contamination are the two major factors resulting in the substandard quality of premium edible oil like extra virgin olive oil (EVOO) produced in food and beverage (F&B) fast-moving consumer goods (FMCG) industries. Current quality assurance methods (e.g., spectroscopy and chromatography) in FMCG involve intrusive sample extraction and ex situ analysis in a laboratory using expensive bulky instrumentation, which is neither integrable inline nor scalable to match the production throughput. Such techniques do not meet the industrial requirements of in situ testing, non-intrusive analysis, and high throughput inspection (100% product verification) leading to food loss and package waste from unwanted batch rejects. Herein, a low-cost electrical approach based on capacitance is proposed to show the proof of concept for screening EVOO-filled containers non-invasively for adulteration without any sample extraction by capturing the differences in the dielectric properties of mixed oils. The sensor system displayed a fast response (100 ms) and low detection limits for different adulterants (olive oil (32.8%), canola oil (19.4%), soy oil (10.3%) and castor oil (1.7%)), which is suitable for high-throughput (>60 sample/min) screening. Furthermore, a low-cost automated system prototype was realized to showcase the possibility of translating the proof of concept for possible scaling up and inline integration.

Keywords: non-invasive; capacitance; adulteration; edible oil; FMCG

check for updates

Citation: Salila Vijayalal Mohan, H.K.; Aung, P.P.; Ng, C.F.; Wong, Z.Z.; Alexander Malcolm, A. Rapid Non-Invasive Capacitive Assessment of Extra Virgin Olive Oil Authenticity. *Electronics* **2023**, *12*, 359. https://doi.org/10.3390/electronics12020359

Academic Editor: S. M. Muyeen

Received: 16 November 2022
Revised: 17 December 2022
Accepted: 8 January 2023
Published: 10 January 2023

Copyright: © 2023 by the authors. Licensee MDPI, Basel, Switzerland. This article is an open access article distributed under the terms and conditions of the Creative Commons Attribution (CC BY) license (https://creativecommons.org/licenses/by/4.0/).

1. Introduction

Quality assurance (QA) in the food and beverage (F&B) industries is of paramount importance to brandish brand integrity and product quality. QA is the foremost boundary between consumers and false foods. It ensures the delivery of high-quality products for consumers and forestalls producers from falsifying claims about product quality. A notable industry that thrives on high-speed mass production like no other is the F&B fast-moving consumer goods (FMCG) industry. Yet, amidst the industry's battle to keep up with a rapidly evolving and expanding consumer base, quality is still at its core. Food adulteration involves lowering food quality by either replacing its major constituents with inferior alternatives or removing major ingredients from the food item. Adulterants are any materials that make the food sub-standard or misbranded or contain extraneous matter [1]. Besides intentional adulteration, storage, mixing and filling conditions in production affect the food quality and ingredient composition. Implementation of quality control tests at high speeds in FMCG supply chains is a major challenge. This has garnered monumental interest in cost-effective yet cutting-edge inspection technologies by both producers and food inspection agencies alike to check for the authenticity of food products at high speeds.

Extra virgin olive oil (EVOO) is a prominent example of a high-value FMCG product. Having an impressively low free acidity of not more than 0.8% (*m*/*m*), EVOO is markedly

the most nutritious and healthiest oil [2], thereby creating a remarkably huge demand and generating market revenue of 1410.2 million USD in 2020, which is projected to further rise to 1465.6 million USD by 2026 [3]. Such in-demand products incite the producers to adulterate EVOO, consequently making EVOO one of the leading types of food that experiences adulteration [4]. When intentional, it is usually done to illicit monetary gain and thus, is known as economically motivated adulteration (EMA) [5]. In the case of EVOO, common adulterants include olive oil (free acidity of less than 1% (m/m)), soy oil, castor oil, and canola oil. Adulteration cost the European Union about 4 million Euros per year [6]. Besides the economic loss, adulteration oils could lead to poor nutritional quality and have major health implications due to the presence of allergic, genotoxic and/or carcinogenic compounds. The other form of loss in edible oil authenticity arises from cross-contamination in processing lines. Oils of similar nature are subjected to processing in the same feedlines after cleaning to save on the cost of constructing new lines and maintain sustainability by adopting a smaller machinery footprint. Additionally, passage through multiple lines for storage, filling, treatment, and dispensing could affect the oil authenticity and introduce unwanted foreign matter. Therefore, the detection of edible oil adulteration is crucial for maintaining food quality and safety.

In general, olive oil is mainly composed of oil fraction and non-oily fraction. The oil fraction is the major portion constituting 98–99% of the total oil. It consists of triglycerides containing monounsaturated fatty acids (MUFA, 55–85%) such as oleic acid [7]. It also contains palmitoleic acid; saturated fatty acids (12.7%), such as palmitic, stearic, and arachidic acids; and polyunsaturated fatty acids (10.1%), including linoleic and linolenic fatty acids. The non-oil fraction contains smaller amounts of minor compounds (1–2%) such as fatty alcohols [8], sterols [9,10], waxes [11], tocopherols [12,13], phenolic compounds [14,15], carotenes and chlorophylls [16,17], n-alkanes and n-alkenes [18] and volatiles [19], which also determines the organoleptic characteristics of olive oil. The antioxidant properties of olive oil are linked to the radical scavenging actions of phenolic compounds such as hydroxytyrosol and oleuropein, which reduce the formation of superoxide anions, neutrophil respiratory burst, and hypochlorous acid thereby lowering the risk of coronary heart disease and cancer associated with the Mediterranean diet [20]. The high levels of unsaturated fatty acids in olive oil improve the lipid profile by reducing the low-density lipid (LDL)/high-density lipid (HDL) ratio in humans. The resistance against the oxidation of LDL by phenolic compounds helps in preventing ischemic heart disease besides improving endothelial function needed for improving the hemostatic system in hypercholesterolemic individuals [21]. Monounsaturated fatty acids like oleic acid induce a positive effect on natural killing cell activity by boosting the immune system [22]. Olive oil increases the concentration of gastrointestinal hormones, which in turn act on the synthesis or secretion of enzymes and other constituents of the digestive juices, thereby promoting faster absorption and metabolism [23]. High oleic acid content has a beneficial effect in curing fatty liver diseases by reducing the accumulation of triacylglycerols in the liver, improving postprandial triacylglycerols glucose, and glucagon (like peptide-1) responses in insulin-resistant subjects, and upregulating glucose transporter-2 expression in the liver [24].

To avail of the maximum nutritional benefits of olive oil, the olive oil quality needs to be of the highest order. This is possible only by controlling both pre-harvest and post-harvest factors. Several pre-harvest factors such as cultivar, edaphoclimatic conditions, environmental conditions, pedalogic conditions, tree age, treatment, fruit ripening and harvest time influence the olive oil quality. For example, the highest content of campesterol, cholesterol, β-sitosterol, and total sterol was detected in Picholine cultivar [9]. Picholine Marocaine cultivar done at 600–900 m altitude showed that the chlorophyll and carotenoids content gradually increases, which is nutritionally preferable [25]. In general, olive flowering requires spring temperatures, growth and development need high temperatures and olive fruit ripening needs heavy rain [26]. Pedologic (sandy, clay, stony, limestone, gypsum and brown soil) conditions influence the α-tocopherol, the sterols composition and the volatiles of the olive oils [27]. Total phenol content is influenced by the age of the tree,

and 30–50 years-old olive trees showed the highest phenol content compared with 10–30 years old trees [25]. The phenols and o-diphenol contents of the oils decrease during fertilization treatments [28]. Boron alters the biochemical functions of phenylalanine ammonia-lyase, peroxidase and polyphenol oxidase activities [29]. Linoleic acid increases during ripening due to oleate desaturase that changes oleic acid to linoleic acid in the olive [30]. Some of the post-harvest factors including fruit storage, leaf removal and fruit washing, fruit crushing, oil extraction systems and oil storage also influence the olive oil quality. Storage of more than 24 h is not recommended between harvesting and processing of olive fruits because longer storage time may hydrolyze the triglycerides to free fatty acids with the action of lipases, in the presence of moisture [31]. Leaf discards used in olive fruit harvesting raise the degree of green color, which gives an organoleptic sensation (color, aroma and taste) [32]. The recommended olive crushing time is 20–30 min because crushing the fruit within this time window produces less peroxide and prolonged crushing could degrade the quality of the olive oil [33]. During storage in plastic containers, reactions occur between oxygen and the unsaturated fatty acids in olive oil occur thereby degrading its quality over time [34]. Pressure, centrifugation and percolation are used for olive oil extractions in olive oil mills from a paste form. Olive oil extraction using natural decanting is time-consuming, laborious and may cause contamination whereas centrifugation reduces time, labor and contamination [33].

Among the several grades of olive oil defined by the European Commission [35] and the International Olive Council (IOC) [36], EVOO is considered the best quality olive oil since is obtained directly from the olive fruit by mechanical or other physical processes without altering oil properties. EVOO has a free acidity, expressed as oleic acid, of not more than 0.80 g per 100 g and the other physico–chemical and organoleptic characteristics correspond to those fixed for this category in this standard [37]. Olive oil obtained by blending refined olive oil and virgin olive oil other than lampante olive oil, having a free acidity content, expressed as oleic acid, of not more than 1 g per 100 g, forms regular olive oil [37]. Due to the premium quality, the price of EVOO is the highest among different grades and is vulnerable to adulteration. Conventional methods such as Fourier transform-infrared (FTIR) spectroscopy [38], near-infrared (NIR) reflectance spectroscopy [39], Raman scattering spectroscopy [40], nuclear magnetic resonance (NMR) spectroscopy [41], high-performance liquid chromatography (HPLC) [42] and gas chromatography (GC) [43] are widely used for edible oil authenticity assessment. These techniques rely on sample extraction from packaged products and offline analysis in a laboratory to identify the chemical composition, fatty acid content, etc. Such offline methods are expensive because of the sophisticated instrumentation that requires a high level of expertise for data analysis and interpretation. This is further compounded by the high implementation cost for large-scale adoption and low inspection throughput due to random sampling, which is not attractive for inline monitoring. In addition, unsealing the packages/containers for sample extraction leads to food loss and package waste generation affecting environmental sustainability [44]. The absence of a reliable in situ oil quality/authenticity monitoring system in conjunction with the drawbacks of the current methods are the motivating factors to seek other rapid low-cost non-destructive evaluation systems to assess edible oil quality. The exponential progression in high-speed electronics and sensor technologies opens avenues to seek alternative non-destructive technologies in the spectrum of food quality checking. The desirable characteristics of such a system are as follows: (i) cost-effectiveness, (ii) high-speed sensing, (iii) in situ placement, (iv) non-intrusiveness, and (v) reduced equipment footprint for seamless inline integration.

Recently, dielectric spectroscopy, a technique which provides dielectric information of a medium as a function of frequency, as a screening tool for authenticity check of edible oils has garnered interest because different fatty acid compositions manifest distinguishable behavior across the electromagnetic spectrum [45]. Dielectric spectroscopy is a closely related technique used to study the response of a sample via the interaction of an external field with its electric dipole moment within a broad frequency range. It is used to estimate

the dielectric permittivity of a material as a function of frequency. Unlike the infrared spectrum used in Raman (0.3 THz–120 THz) [46], FTIR (12–120 THz) [47], and NIR spectroscopy (118–384 THz) [48], dielectric spectroscopic characterization covers a relatively lower frequency range (few MHz to GHz); which is economically viable for low-throughput offline inspection when compared with the other spectroscopic methods [49]. Despite its attractive features, dielectric spectroscopy faces several challenges for deployment in an inline high-throughput inspection environment. Being a wide-range frequency response method capable of measuring the dielectric permittivity directly, the operational frequency range should be high (MHz-GHz) to induce polarization. Such high-frequency analysis requires an expensive microwave probe station and/or bulky benchtop vector network analyzer (VNA) equipment, which limits in situ inspection and large-scale implementation in a high-throughput inspection setting such as FMCG. Moreover, to estimate the dielectric properties accurately, the electric field needs to be concentrated near the material under test. Consequently, the dielectric probe is in proximity or contact with the sample to reduce the influence of package/container dielectric effects. The current research on portable dielectric spectroscopy-based sensors is limited to intrusive offline testing using concentrated high-frequency waves for a small sample volume (few uL) and/or contact analysis from a dedicated ex situ inspection region [50,51] and no reports on in situ and non-intrusive testing of finished packaged goods are available. However, the promising aspects of dielectric spectroscopy give the incentive to pursue an electrical response method, which can overcome the current drawbacks of dielectric spectroscopy.

Capacitance ($C = \varepsilon_r \varepsilon_o A/d$), is one quantity, which is a function of the material property (dielectric constant or relative permittivity of the material, εr and εo is the permittivity of free space = 8.85 $\times$ 10–12 Fm^{-1}), the material dimensions (A, electrode area traversing the field), and the distance (d) from the material under test, that offers an electrical readout capable of overcoming the aforementioned drawbacks of traditional methods and dielectric spectroscopy [52–54]. Capacitive sensing distinguishes material types and physical changes to the material under test, allows contactless operation, provides adjustable sensing depth, is low-cost, fast and requires low power [55–57]. The close correlation between capacitance and dielectric property could be extrapolated to both quantitatively and qualitatively assess the deviation in the authenticity of edible oils via blending with low-grade alternatives. Such oil mixtures possess a different dielectric characteristic compared with authentic oils, which is readily distinguishable via indirect capacitance profiling at a single frequency without requiring expensive probes and wide-range frequency characterization to estimate the actual dielectric constant. Hitherto, both capacitive sensing and dielectric spectroscopy, have been explored for food/oil quality characterization [58,59]. Food spoilage detection [60], water content estimation in edible oils [61], moisture measurement in food [62] and adulteration in olive oil [63,64] are some of the applications reported using offline capacitive/dielectric analysis on extracted samples. Albeit in its infancy, capacitance-based non-destructive testing of food container/package quality has shown great potential for further exploration [65–68]. This provides the incentive to extrapolate the concept of capacitance for adulteration detection. To the best of our knowledge, the proposed capacitive approach herein is novel for direct through-container screening of EVOO for authenticity check without requiring oil extraction from a sealed container. In general, the proposed detection method offers an economical pathway for high-throughput non-invasive edible oil inspection warranting further research for adulteration detection. Furthermore, capacitive sensing offers bespoke electrode designs, sensing topologies and sensor placement configurations with controllable field penetration depth and strength to accommodate end-product aesthetics and overcome any mechanical constraints during customized inline integration. The through-container testing scheme does not require any oil sample to be extracted for offline analysis, which prevents unwanted waste generation (food and package) from the disposal of tampered containers, which is contrary to the existing offline industrial solutions.

In this work, a portable low-cost capacitance measurement setup comprising two parallelly placed rectangular electrodes demonstrates the feasibility of non-invasive adulteration detection in packaged containers without any form of sample extraction. EVOO-filled containers adulterated to varying degrees with different adulterants served as the dielectric medium between the electrodes. The electrostatic field between the electrodes generates capacitance signals of varying strengths depending on the degree of adulteration and the type of adulterant. The proof of concept was further translated into a small-footprint automated preliminary prototype targeted towards the development of a standalone system with inline integration potential.

2. Materials and Methods

2.1. Preparation of Blended Oils

Several commercially available edible oils were purchased from retail stores including extra virgin olive oil (EVOO, Naturel®, Andalusia, Spain), olive oil (OO, Naturel®, Andalusia, Spain), soybean oil (SOY, FairPrice, Singapore), sunflower oil (SF, FairPrice, Singapore), vegetable oil (VEG, blend of 50% palm oil and 50% soybean oil, FairPrice, Singapore), canola oil (CAN, FairPrice, Singapore) and castor oil (CAS, Ambika, India). EVOO and OO are products of Spain with an expiry date in 2025. All other oils were products of Singapore. No information on the harvest and/or geographical origin was provided unless specified otherwise. All oils were purchased and tested in 2022. Commercial vegetable oils are blended mixtures of palm oil with other edible oils for stability since palm oil is solid below 40 °C. EVOO was spiked using 4 common adulterants (OO, SOY, CAN and CAS) to make binary mixtures with 6 degrees of adulteration (2.5%, 5%, 10%, 20%, 40% and 60% (*v*/*v*)). Plastic containers made of polyethylene terephthalate (PET) with a wall thickness of ~1.2 mm were used for the sensing experiments. 15 mL oil volume was used throughout the study unless stated otherwise.

2.2. Sensing Setup

Figure 1 shows the experimental setup, sensing configuration and sensor electrode design used in this study. Rectangular-shaped sensor electrodes were designed in-house using printed circuit board (PCB) design software (EasyEDA, JLCPCB, Shenzhen, China) and outsourced for fabrication on FR4 PCB substrates (JLCPCB, China). Two electrodes spaced 27 mm apart were connected to two excitation terminals (INA and INB) of a capacitance sensing module (FDC2214EVM, Texas Instruments, Dallas, TX, USA). The FDC214 capacitance board uses a sinusoidal excitation signal with a default frequency of 5 MHz and a peak-to-peak voltage (*Vp-p*) of 1.8 V and is operated in a differential sensor topology (refer to Section 3.4), where two terminals are excited by the same signal to produce a strong sensing field necessary to cover the entire diameter (sensing depth) of the container with a non-polar liquid like oil [69].

2.3. Capacitance Measurements

Real-time capacitance data was logged using Sensing Solutions EVM GUI (Texas Instruments, Dallas, TX, USA). All measurements were done in a laboratory ambience (room temperature (RT) ~25 °C and relative humidity (RH) ~60%) unless stated otherwise. Statistical analysis, data plotting, linear fitting and hypothesis testing were performed using OriginPro software (v2019b, Northampton, MA, USA). To demonstrate measurement reproducibility and repeatability, at least 6 containers were tested per container/oil sample with 3 repeats for a total of ~12 s (4 s per sample), thereby yielding ~300 data points (100 ms sampling rate) per oil type unless stated otherwise. For sensor characterization, capacitance responses to all oils were recorded before adulteration experiments. The responses were obtained using the relative capacitance ($\Delta C/C_O = (C - C_0)/C_0$), with air as the baseline (blank), where C_0 and C are capacitances of the sensor in air and with container (filled and unfilled), respectively.

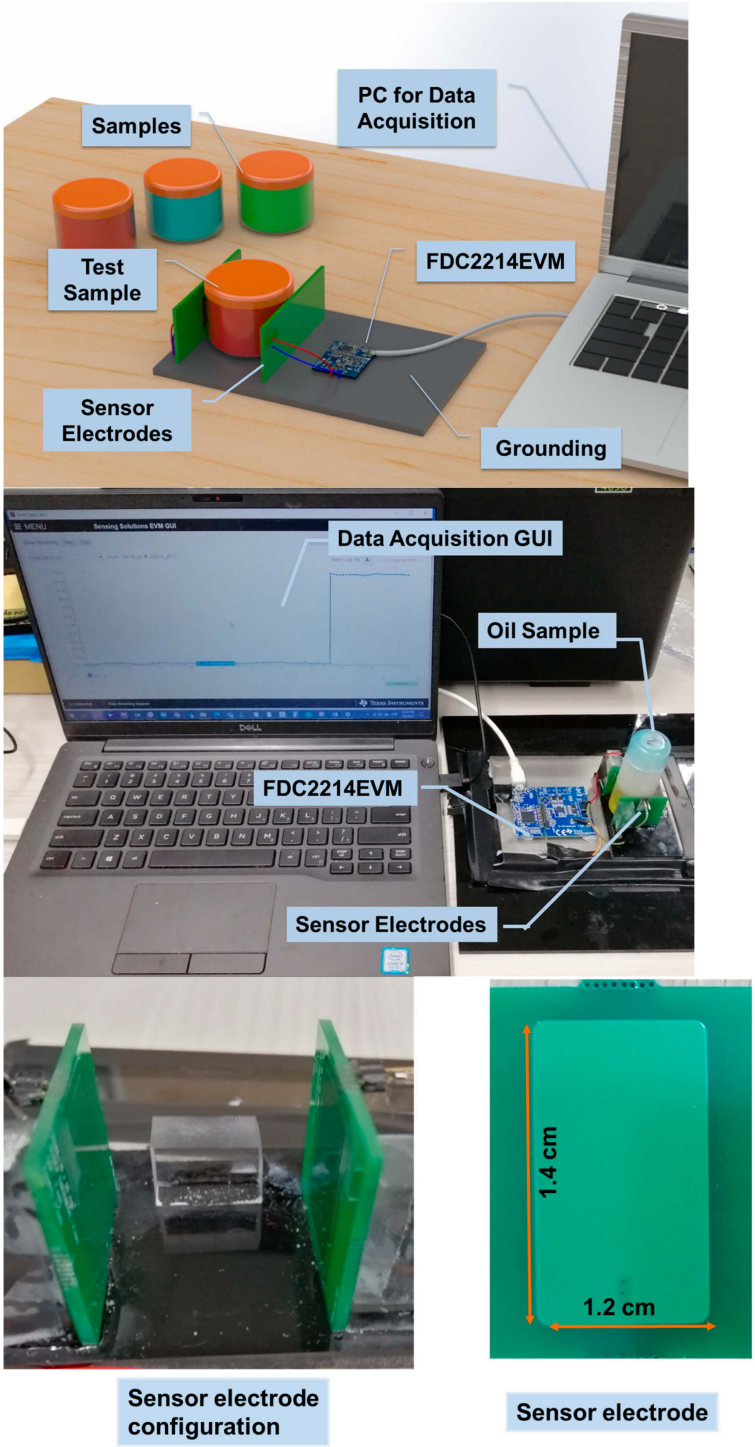


Figure 1. Capacitance-based edible oil adulteration testing setup: Schematic of the experimental setup (**top**) and the corresponding photograph (**middle**). Photographs of the parallel plate sensor configuration (**bottom-left**) and PCB fabricated rectangular-shaped sensor electrodes (**bottom-right**).

To obtain the sensor calibration curve for adulteration tests, four commonly used adulterant oils, namely, OO, SOY, CAN, and CAS were mixed with EVOO in varying proportions and evaluated. The relative capacitance ($\Delta C_{EVOO}/C_{EVOO} = (C_{AO} - C_{EVOO})/C_{EVOO}$) of the calibration curve was calculated using EVOO as the reference (blank), where C_{AO} and C_{EVOO} are capacitances of EVOO oil (blank) and adulterated EVOO (blending with OO, SOY, CAN, or CAS), respectively. The slope of the sensor calibration curve (($\Delta C_{EVOO}/C_{EVOO}$)

vs. the degree of adulteration (%)) curve gives the sensor sensitivity (s). The limit of detection (LOD) is given by $3\sigma_b/s$, where σ_b is the standard deviation of the blank EVOO measurements [65,66,70,71]. A linear fit ($y = a + bx$, where b and a represent the slope s and the y-axis intercept, respectively) to the calibration curve gives the correlation coefficient of determination (R^2).

3. Results and Discussion

3.1. Sensor Characterization

In general, the polarizable nature of the liquid under test dictates the signal strength. For example, liquids with high water content (diploes) are expected to have very high capacitive signals due to high dielectric constant values (ε_r ~80) (e.g., milk, water, juice, etc.) while insulating liquids (e.g., oil, honey, etc.) devoid of water molecules/dipoles are not easily polarizable and have very low dielectric constant values ($\varepsilon_r < 5$) [72,73], which makes sensing mixed oils difficult, and more so when carried out non-intrusively because of the thick insulating package material acting as a barrier and reducing the denser electric field lines (near the electrode surface) from accessing the actual material under test (oil). Sensor characterization was performed to assess the sensor stability in air before actual adulteration testing to ensure that the unblended oil responses are separable, to begin with. The mean capacitance (μ) ± standard deviation (σ) of the capacitive sensor in air obtained from a recording of 1.5 h was ~55.675 ± 0.003 pF (air). The relative standard error expressed in percentage ($\sigma_{rse} = \sigma/\mu\sqrt{n}$), n = 5664) was estimated to be ~0.006%. (Figure 2a). The low error percentage confirms the stability of the recordings at such a high data acquisition speed, which is promising for implementation in high-throughput quality check scenarios in FMCG lines. Figure 2b shows the real-time capacitance of a sensor in air, with an empty container and unblended oil-filled containers. The average capacitance ($\mu \pm \sigma$) of the sensor increased from 55.696 ± 0.0004 pF to 55.735 ± 0.0004 pF upon insertion of an empty container, and to 55.983 ± 0.064 for unblended oil-filled containers in the capacitive field. The relative standard error (σ_{rse}) estimated for air, unfilled, EVOO, OO, SOY, SF, VEG, CAN, and CAS, was 0.007%, 0.007%, 0.004%, 0.004%, 0.001%, 0.001%, 0.002%, 0.001% and 0.002%, respectively. Figure 2c shows the relative capacitance ($\Delta C/C_0$) expressed in % for unfilled and unblended oil-filled containers with air as the baseline. The sensor displayed a positive capacitance change upon placing both empty and filled containers in the inter-electrode gap in the following order air < unfilled < EVOO < OO < SOY < SF ≈ VEG ≈ CAN < CAS. $\Delta C/C_0$ of unblended oil-filled containers is at least a 6-fold (~0.52 ± 0.12%) greater compared to unfilled containers (~0.06%), which signifies the higher dielectric contribution of oil towards the overall capacitance compared to the container (refer to Section 3.4 and 3.5) since the container material has a very lower dielectric constant (~2–3 for PET [67,68]) and container wall thickness (~1.2 mm).

$\Delta C/C_0$ for all unblended oils are substantially greater (ranging from 487 to 974-fold) compared to their relative standard errors (ranging from 0.001% to 0.007%), and 87 to 620-fold greater than the relative standard error of blank (air). Furthermore, $\Delta C/C_0$ of OO, SOY, SF, VEG, CAN, and CAS, with respect to EVOO, increased by ~0.012%, ~0.197%, ~0.212%, ~0.209%, ~0.215% and ~0.355%, respectively. Even after replacing the baseline reference as EVOO, the observed responses for all oils remained significantly greater (3 to 230-fold) than their above-stated individual relative standard errors, and at least 3 to 86-fold greater than the relative standard error of EVOO (blank). Hence, for actual adulteration calibration (Section 3.5), EVOO replaced air as the blank measurement (baseline reference). Additionally, statistical hypothesis testing performed using two t-test confirms that the results are statistically significant with $p < 0.01$ for oil identification and classification (refer to Figure S1 in Supporting Information (SI)). Overall, the sensor characterization underscores the ample capacitive signal strength and the good separability between EVOO and adulterant oils, which is crucial for oil-type classification and adulteration detection.

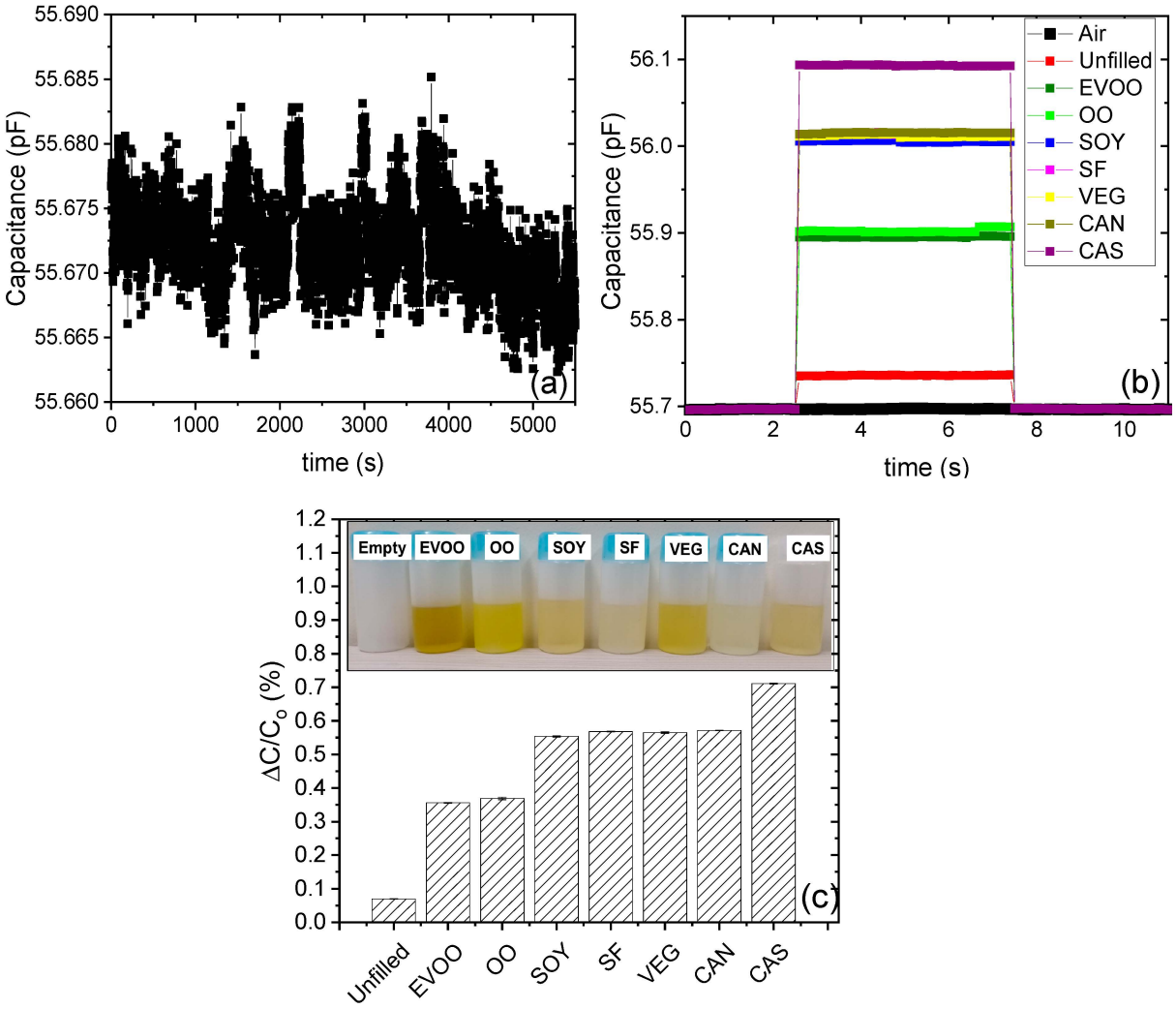


Figure 2. Sensor characterization: (**a**) Real-time capacitance of the sensor (in air) recorded for ~1.5 h. (**b**) Capacitance vs time and (**c**) $\Delta C/C_0$ ($\pm\sigma$) of unfilled containers and unblended oil-filled containers, respectively, expressed in percentage. Extra virgin olive oil−EVOO, olive oil−OO, soybean oil−SOY, sunflower oil−SF, vegetable oil−VEG, canola oil−CAN and castor oil−CAS.

3.2. Sensor Validation

The capacitance testing performed using FDC2214EVM was calibrated against a standard LCR system (Keysight, Impedance Analyzer, E4990A, 20 Hz to 30 MHz) to validate the obtained observed responses and trend. E4990A gives the absolute capacitance value of capacitive sensors whereas FDC2214 is intended for monitoring capacitance changes in applications. The absolute capacitance values of the sensor connected to FDC2214EVM and E4990A are expected to be different due to inherent system baseline differences from internal circuit configurations. A quick test showed that the change in capacitance obtained using FDC2214 evaluated using a standard 50 pF ceramic capacitor was found to be close to the absolute capacitance measured using E4990A (refer to Figure S2 in SI). Hence, the relative capacitance ($\Delta C_{EVOO}/C_{EVOO}$) was used for comparison and validation of the sensing methodology and system. The cumulative capacitance responses from E4990A for all unblended oils with EVOO as blank showed good response and separability as seen in Figure 3, which is consistent with the earlier observed trend. Unlike the E4990A, which can perform the cable length compensation correction during calibration to accommodate the 1 m probe cable length, the FDC2214EVM is affected by the stray parasitic capacitance of

the wirings to the terminals leading to slightly lower response levels. Nevertheless, the closeness of the observed responses using both systems validate the sensing methodology.

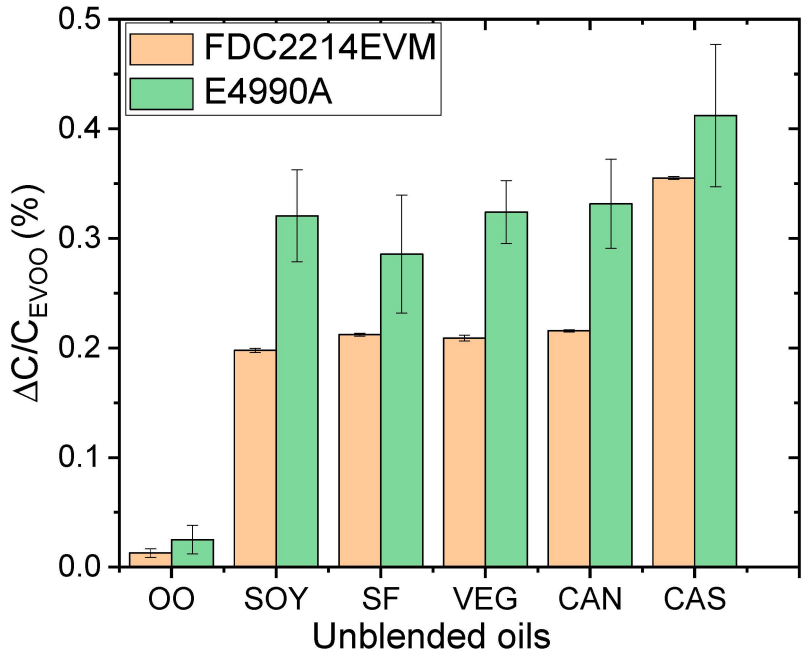


Figure 3. Sensor validation using E4990A (excitation frequency of 5 MHz and $V_{p\text{-}p}$ of 1 V): Bar plot comparing $\Delta C_{EVOO}/C_{EVOO}$ ($\pm\sigma$) obtained using FDC2214EVM and E4990A for all unblended used in this study. Olive oil—OO, soybean oil—SOY, sunflower oil—SF, vegetable oil—VEG, canola oil—CAN and castor oil—CAS.

3.3. Sensing Methodology Optimization

The optimization of the capacitive sensing protocol is important to achieve good capacitive signal strength with observable separability between EVOO and adulterant oils before its extension to authenticity checking using binary solution blends. Such optimization is attained through experimental testing to find the right concoction of sensor configuration, sensing area and operational frequency.

FDC2214 allows multi-channel measurements (up to four) with each channel having two terminals (INA and INB) for excitation, thereby allowing two modes of operation for any given channel: (i) single-ended mode, where INA/INB is connected to one electrode and another electrode is connected to FDC2214 ground terminal; and (ii) differential configuration, where each sensor electrode is connected to one excitation terminal (INA and INB) of the corresponding channel. The single-ended configuration offers a greater sensing range but with reduced sensitivity compared to the differential configuration for a given total sensor plate area, thereby making it useful for displacement-based sensing applications [69]. On the other hand, the differential configuration produces a stronger sensing field but with a reduced sensing range, which is attractive for material property analysis (e.g., liquid level sensing) [69]. This was verified experimentally in Figure 4a, which shows that $\Delta C_{EVOO}/C_{EVOO}$ of adulterant oils are much higher and separable from EVOO for the differential mode vis-à-vis single-ended mode, which affirms that a stronger field encompassing the oil is responsible for the observed behaviour. Hence, a differential configuration capable of generating a strong electrostatic field was adopted in this work to detect low dielectric changes from oil mixing. The electrode area determines the strength of the electric field, coverage of the material under test and the penetration depth of the sensing field. Experiments were conducted to study the influence of electrode area and downselect the optimal electrode area to elicit the maximum response as shown in Figure 4b using four different electrode areas (A) (A1—100 mm^2, A2—168 mm^2, A3—468 mm^2

and A4—900 mm^2). Reducing the electrode area decreases the electric field strength and penetration depth rendering it difficult to distinguish the oils. On the other hand, increasing the electrode area beyond a threshold lowers the overall response since most of the electric field dissipates onto the container's empty overhead space and ambience (air has a very low dielectric constant), resulting in poor coverage of the actual contents. To develop low-cost yet high-speed detection systems for screening non-polar liquids, the selection of the correct excitation frequency range is critical. Most of the commercially available capacitance development boards offer an excitation frequency in the range of 10–100 kHz [65,66]. However, such low frequencies are insufficient to generate a strong electric field for assessing non-polar liquids. To demonstrate that a higher frequency is desirable for testing non-polar liquids, a comparison of the raw capacitances of the two FDC boards is shown in Figure 4c. FDC2214EVM with higher noise immunity and a higher frequency of operation (5 MHz) showed clear separability between the unblended oils while FDC1004EVM operating at a lower frequency (25 kHz) failed to show any distinction between the oils, which is consistent with the literature [64].

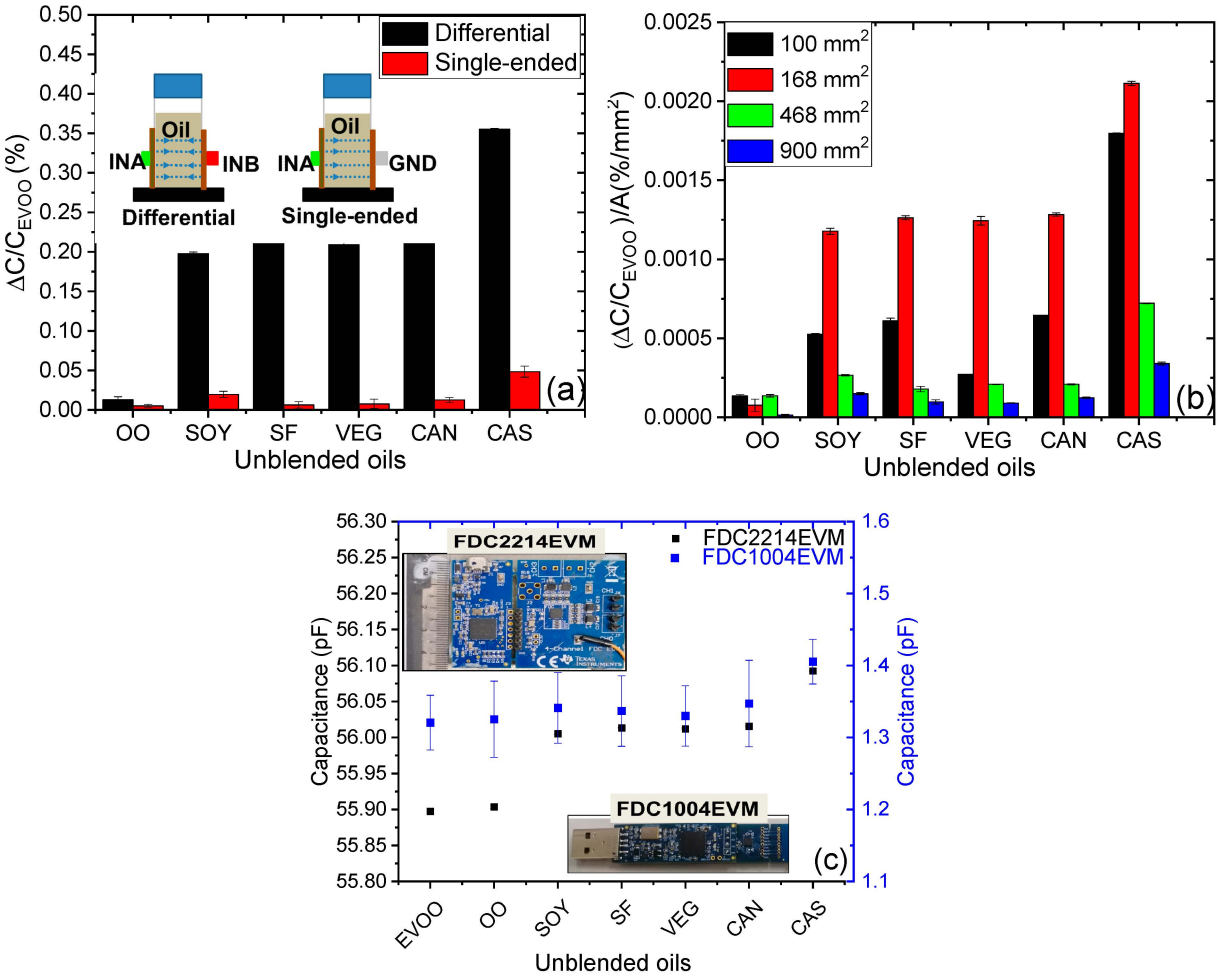


Figure 4. Sensing methodology optimization: (**a**) $\Delta C_{EVOO}/C_{EVOO}$ ($\pm\sigma$) for single-ended vs. differential FDC2214 sensor configuration (schematic of sensing configuration in inset); (**b**) $\Delta C_{EVOO}/C_{EVOO}$ ($\pm\sigma$) (Normalized by sensor area) vs. electrode area; (**c**) Absolute capacitance ($\pm\sigma$) comparison plot for FDC1004 and FDC2214 (photographs of FDC2214 and FDC1004EVM in inset Extra virgin olive oil—EVOO, olive oil—OO, soybean oil—SOY, sunflower oil—SF, vegetable oil—VEG, canola oil—CAN and castor oil—CAS.

3.4. Sensing Mechanism

As mentioned earlier, capacitance (C) is related to the relative permittivity or dielectric constant ($\varepsilon_r = \varepsilon/\varepsilon_o$) of the material under test, where ε_o is the permittivity of the free space and ε is the permittivity of the material. Figure 5 shows the schematic of the capacitive sensing working principle for oil adulteration detection. ε_{rB}, ε_{rO}, ε_{rA} and ε_{rAO} denote the permittivity of air, good oil plus container, adulterant oil plus container, and blended oil plus container, respectively, and C_B, C_O, C_A and C_{AO} represent their corresponding capacitances. Since $C \propto \varepsilon_r$, the presence of oil plus container as dielectric (ε_{rO}, ε_{rA}, $\varepsilon_{rAO} > \varepsilon_{rB}$) in the sensing area elevates the output capacitance (C_O, C_A, $C_{AO} > C_B$), where ε_{rB} ~1 (air has the lowest dielectric constant). The permittivity of the adulterant oil (ε_{rA}) dictates the sign of capacitance change (C_{AO}). Adulteration using higher dielectric oil ($\varepsilon_{rA} > \varepsilon_{rO}$) produces a positive change in capacitance ($C_{AO} > C_O$) and vice versa ($C_{AO} < C_O$) for a lower dielectric oil ($\varepsilon_{rA} < \varepsilon_{rO}$).

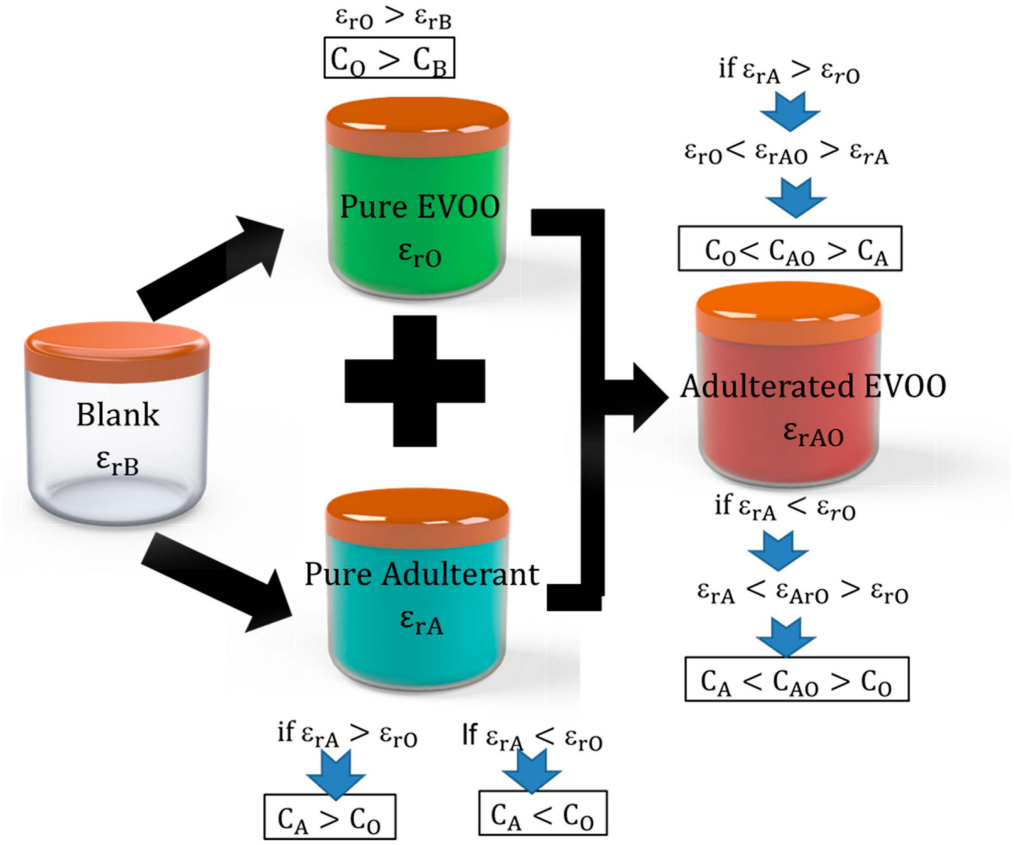


Figure 5. Schematic showing the working principle of capacitive detection of oil adulteration.

3.5. Sensor Response Calibration and Performance

There exists a close correlation between the density and fatty acid unsaturation with the dielectric constant. Table 1 summarizes the dielectric constant, density and dominant fatty acid composition present in the oils used in this study. The density of fatty acids increases in the following order: oleic acid < linoleic acid < ricinoleic acid (Figure 6). In common fatty acids found in oils (oleic acid and linoleic acid), the density increases with the degree of unsaturated bonds, i.e., cis-alkene functional groups (C=C bonds). The density of a substance in the liquid state is largely dependent on the geometry of the constituent molecules and its subsequent effect on the intermolecular forces. The relationship between the asymmetrical structure of the substituent groups across the bond and the overall dipole moment of the fatty acid dictates the degree of polarizability and density. As the number of cis-alkene bonds increases, so does the polarity of the molecule, allowing stronger dipole-dipole, resulting in the molecules packing closer together. Ricinoleic acid has extensive

hydrogen bonding between its molecules lending it its high density. In general, the more mass per unit volume of oil, the more molecules there are to be polarized within the sensing field, leading to a higher dielectric constant. It is to be noted that CAN, VEG, SF and SOY shown in Figure 2c have very close capacitance values even though SOY and SF have higher dielectric constants and densities compared to VEG and CAN. This is due to the presence of both oleic and linoleic acid in significant amounts as opposed to the other oils with a clear dominant fatty acid. In general, the observed capacitance of oils is still in agreement with the density/dielectric property trend shown in Table 1. Since SF and VEG have similar fatty acid composition, dielectric constant, and capacitance response as SOY and CAN, respectively, they were omitted from the adulteration experiments.

Table 1. Dielectric constant, fatty acid content and density of all oils used in this study. Extra virgin olive oil−EVOO, olive oil−OO, soybean oil−SOY, sunflower oil−SF, vegetable oil−VEG, canola oil−CAN and castor oil−CAS.

Property	EVOO	OO	SOY	SF	VEG	CAN	CAS
Dominant unsaturated fatty acids (% m/m)	Oleic acid (55–83%) Linoleic acid (3–21%) [35–37,74,75]	Oleic acid (55–83%) and Linoleic acid (3–21%) [35–37,74,75]	Linoleic (48–59%) and Oleic acid (17–308%) [37,76,77]	Linoleic acid (52–65%) and oleic acid (26–36%) [37,76,77]	Oleic acid (20–29%) Linoleic (27–31%) [37,78,79]	Oleic acid (57–62%) and linoleic (15–22%) [37,76,77]	Ricinoleic (87–90) [80]
Density (kg/L at 20 °C)	0.909 [81]	0.909 [75]	0.931 [82]	0.932 [82]	0.925 [82]	0.917 [82]	0.959 [80]
Dielectric constant (ε_r)	2.81 [83,84]	3.005 [83]	3.020 [85]	3.020 [84]	3.01 [85]	3.015 [85]	4.5 [86]

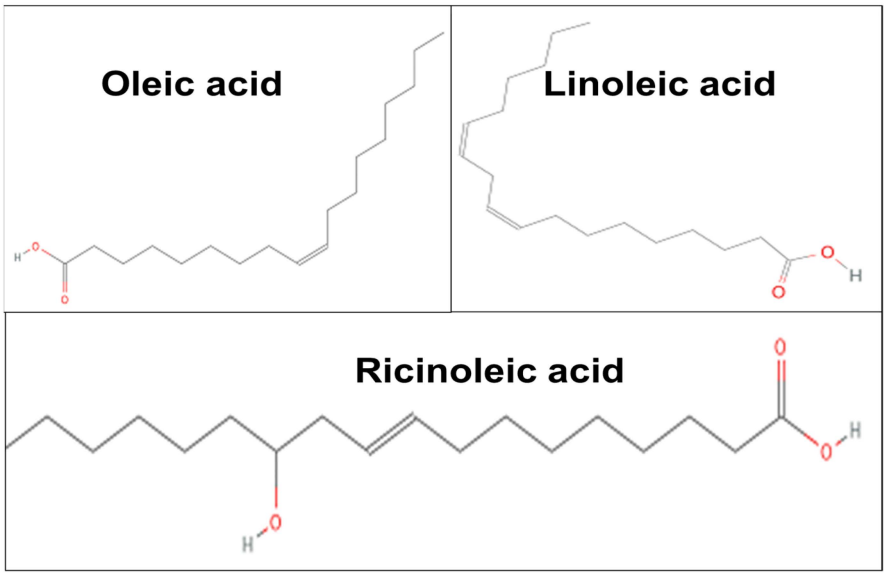


Figure 6. Chemical structure of different fatty acids.

Figure 7a–c shows the sensor calibration plots of binary mixtures generated by spiking EVOO with OO, CAN, SOY and CAS oils to various degrees (2.5–60%). The sensor response ($\Delta C/C$) showed a positive relationship with the degree of adulteration. This is attributable to a combination of increased oil density and dielectric contribution from the adulterant towards the overall capacitance. Table 2 summarizes the sensor performance parameters (s, LOD and R^2) extracted from the linear fitting of the sensor calibration plots in Figure 7 for the different adulterants. The increased composition of denser fatty acids like ricinoleic acid (in CAS) and linolenic acid (in SY) compared to oleic acid (in CL) contributes to the greater oil densification from mixing, which is responsible for the differences in the sensor

sensitivity for the same degree of adulteration. Olive oil with its closeness to EVOO in chemical composition showed the lowest sensitivity and the poorest detection limit making it the hardest adulterant to detect using capacitance.

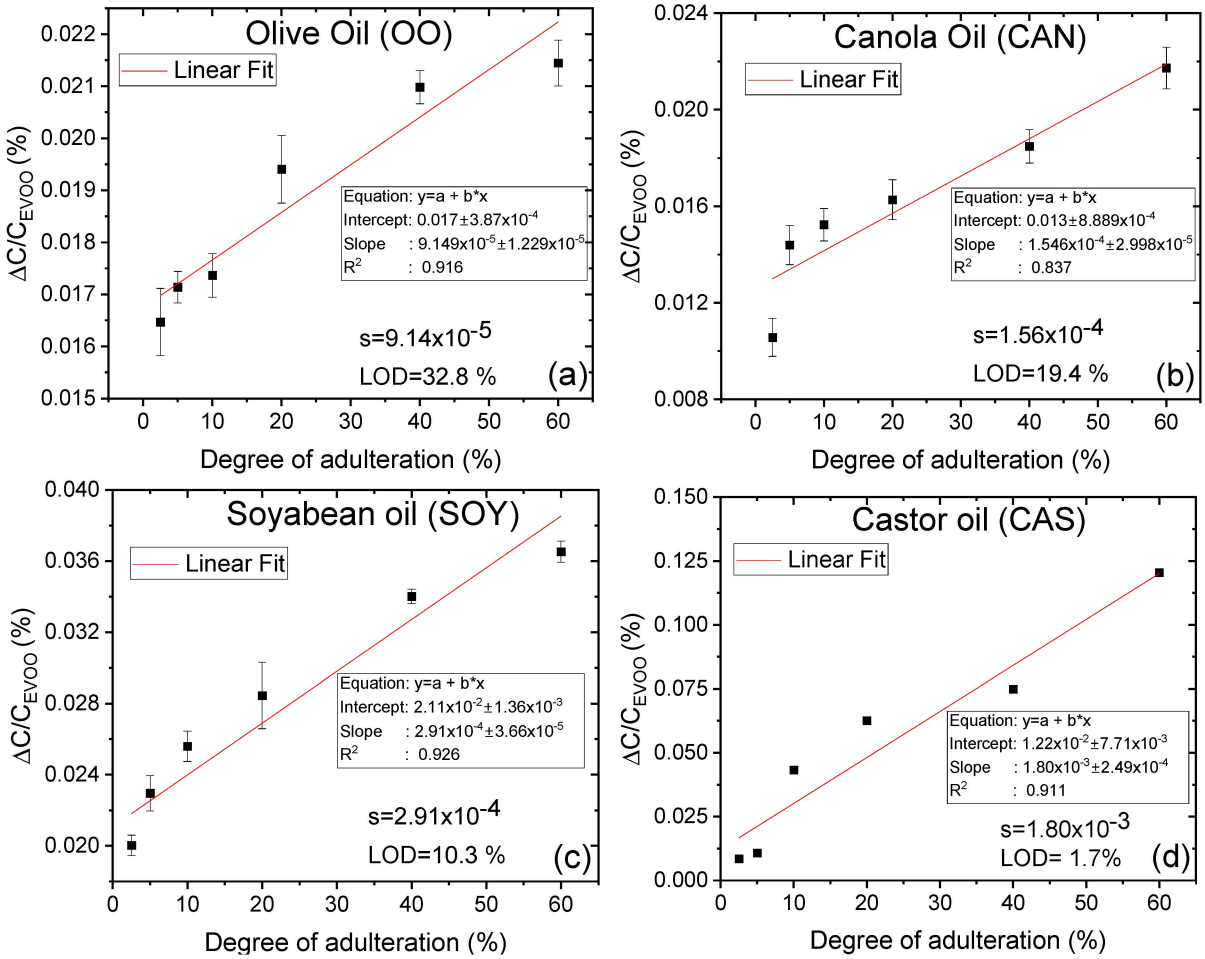


Figure 7. Sensor calibration curves with linear fitting: $\Delta C_{EVOO}/C_{EVOO}$ vs. degree of adulteration (%) in EVOO mixed with (**a**) OO, (**b**) CAN, (**c**) SOY and (**d**) CAS, respectively. Extra virgin olive oil−EVOO, Olive oil−OO, soybean oil−SOY, canola oil−CAN and castor oil−CAS.

Table 2. Summary of sensor performance parameters for EVOO adulteration detection. Extra virgin olive oil-EVOO, Olive oil−OO, soybean oil−SOY, canola oil−CAN and castor oil−CAS.

Sample	Sensitivity (s)	Limit of Detection (LOD) (%)	Correlation Coefficient (R^2)
EVOO + OO	9.14×10^{-5}	32.8	0.918
EVOO + CAN	1.56×10^{-4}	19.4	0.837
EVOO + SOY	2.91×10^{-4}	10.3	0.926
EVOO + CAS	1.80×10^{-3}	1.7	0.911

In general, to minimize variability during batch production in F&B FMCG and ensure the reliability of offline product quality tests, the ambient conditions are kept relatively constant. The testing ambience boundaries were set as air-conditioned (A/C, 25 °C and RH~60%) and non-air-conditioned (non-A/C, 31 °C, RH~90%) ambience, respectively, to closely resemble the offline laboratory and F&B production environment for tropical countries (such as Singapore). The effect of humidity and temperature on the sensor response

was assessed separately. From Figure 8a, at constant humidity (RH~60%), the bare sensor capacitance drift constitutes only a 0.01% change for every 1 °C rise in temperature. Moreover, this change in response occurs in 1.5 h, thereby constituting an almost insignificant change of 1.85×10^{-5}%s^{-1}. A rise in humidity at a constant temperature (25 °C) produces a steeper positive slope in the response from the additional moisture content (dielectric contribution) as shown in Figure 8b. The humidity-induced response albeit higher compared to the temperature-induce response during the same time frame of 1.5 h, is still insignificant since the baseline capacitance drift causes a 0.006% change for every 1% change in RH (3.27×10^{-5}%s^{-1}). The change in total bare sensor capacitance caused by the drift between the two boundary conditions is ~6.48×10^{-5}%s^{-1}. Overall, both humidity and temperature effects on the sensor are slow and have a very small magnitude, which is insignificant compared to oil-induced responses occurring in less than a second from the calibration curves in Figure 7. Hence, the sensor is expected to function without much loss in sensitivity for RH in the range of 60–90% and temperature between 25–30 °C. To further validate the above claims, 60% adulterated oils were tested at different humidity levels. Figure 8c shows the closeness of the $\Delta C_{EVOO}/C_{EVOO}$ values for different RH, which affirms the low impact of external ambience on the sensor response. soybean oil (SOY, FairPrice, Singapore).

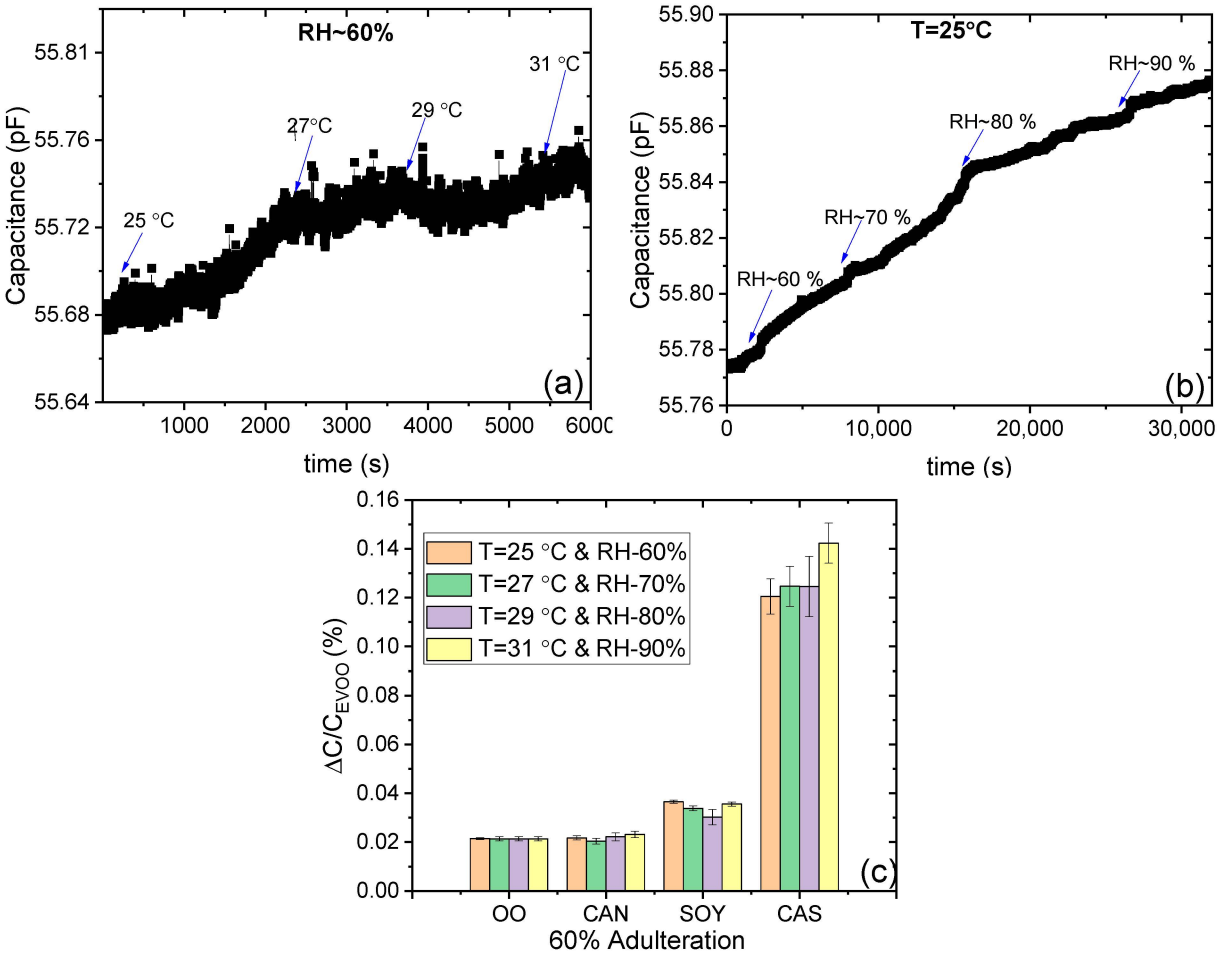


Figure 8. Effect of ambient conditions: (**a**) Real-time capacitance of the bare sensor with increasing ambient temperature and constant RH~60%. (**b**) Real-time capacitance of the bare sensor with increasing ambient RH and constant temperature (25 °C). (**c**) Comparison of $\Delta C_{EVOO}/C_{EVOO}$ ($\pm\sigma$) for 60% adulteration at different temperatures and RH conditions. Olive oil−OO, soybean oil−SOY, canola oil−CAN and castor oil−CAS.

The type of container (material and size) could affect the sensitivity of the sensor. Hence, trials were conducted directly on commercial EVOO containers available in the market to check the efficacy of the method for industrial implementation and further validate the sensing methodology. The commercial EVOO comes in two types of packaged containers, glass (1 L) and PET (2 L) with a container wall thickness of 5 mm and 0.6 mm, respectively. To account for the bigger size of glass (70 mm width), and PET bottle (110 mm width) compared to the small containers (15 mL, 27 mm width) used earlier, two rectangular electrodes with an area of 416 mm^2 area were used in a differential configuration. EVOO and 20%-SOY blended EVOO samples were tested on both containers and compared against the earlier results. Since the sensor area used was different, normalized (by area) relative capacitance (Air/EVOO as blank) was used for comparing the sensor response to container material/blending.

Figure 9a shows the two types of commercial EVOO (Naturel®, Andalusia, Spain), sensor electrode placement configuration and sensor electrode design used for these trials. Figure 9b shows the normalized (by area) relative capacitance comparison (air as blank) of the three types of containers tested in this study. Clearly, the response of the glass bottle increased by 10 to 20-fold compared to the two PET bottles, which is attributable to the combination of greater wall thickness (5 mm) and higher dielectric constant (3–4) of glass compared to PET bottles (0.6 mm and 1.2 mm) with a dielectric constant of 2–3. Furthermore, the 2 L bottle response was 50% lower compared to the 15 mL vials due to the reduction in container wall thickness by half. The thicker glass container and higher dielectric constant of glass is expected to lower the sensor response to adulteration detection since the electric field strength is decaying with distance and the effective electric field reaching the contents inside is diminished. Similarly, the reduced thickness of the 2 L PET bottle is expected to increase the response to blending as more field is penetrating the oil contents. Figure 9c,d show the increase in sensor response upon blending as discussed under Sections 3.4 and 3.5. Figure 9d confirms the above-mentioned postulations, wherein the sensor response to 20%-SOY blending was lowest in glass bottles and highest in the 2 L-PET bottles when compared to the 15 mL PET containers. This reduction in sensor response for glass bottles could be easily circumvented by increasing the electrode length (vertically) to enhance the penetration depth of the sensing field.

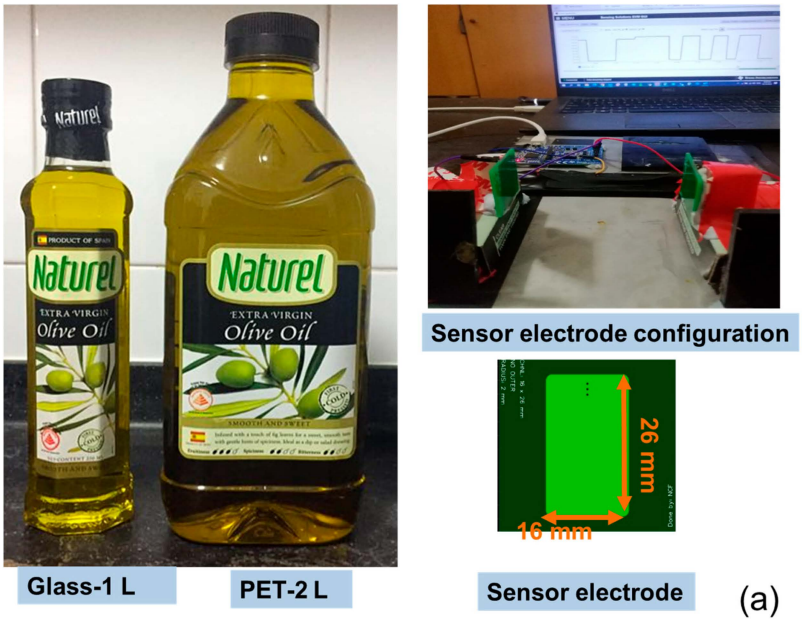


Figure 9. *Cont.*

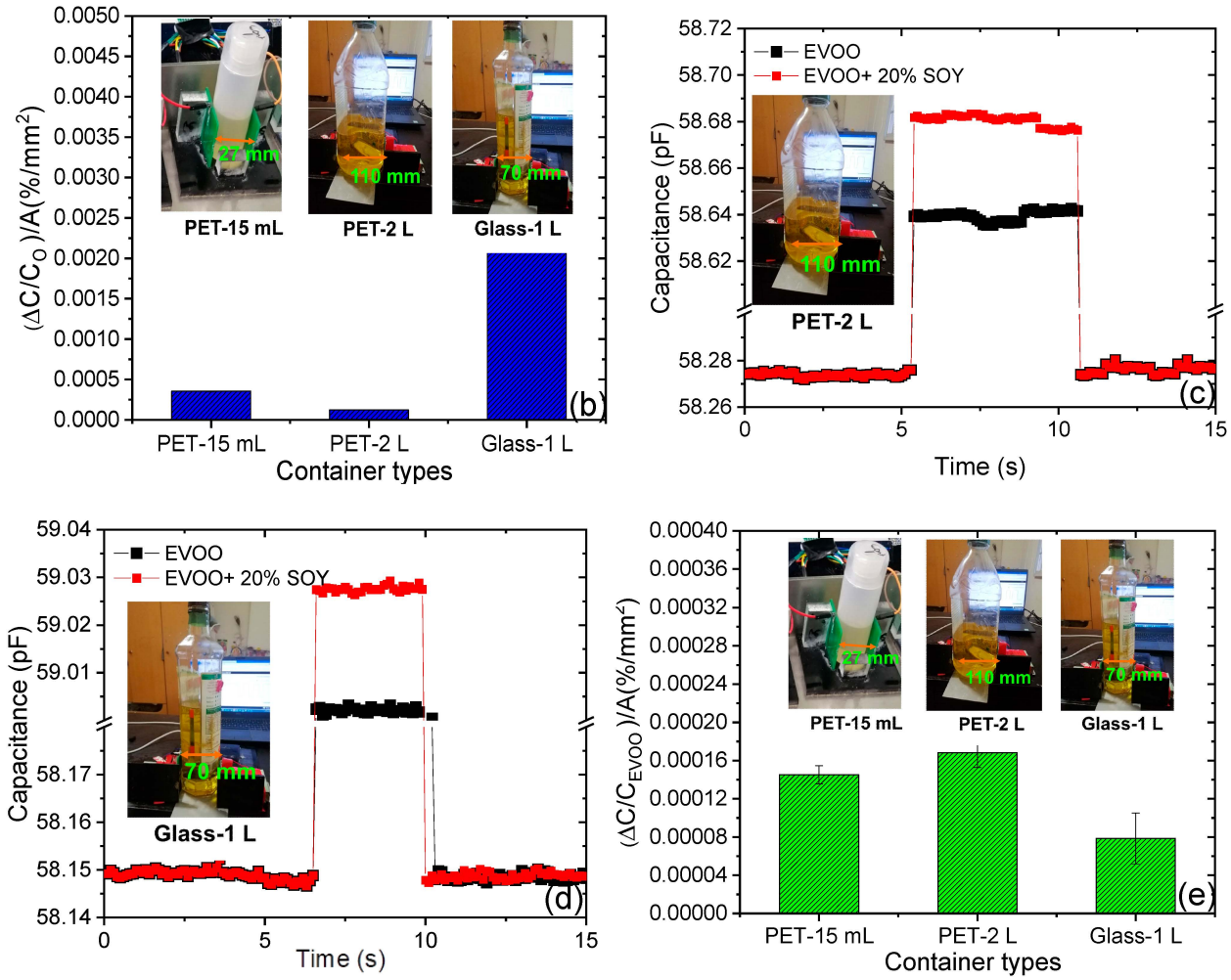


Figure 9. Effect of container type: (**a**) Photograph of the commercially purchased EVOO containers (**left**), photographs of the parallel plate sensor configuration (**top-right**) and PCB fabricated rectangular-shaped sensor electrodes (**bottom-right**). (**b**) $\Delta C/C_O$ ($\pm\sigma$) (normalized by sensor area) vs. container type. Capacitance vs time plot of (**c**) 2 L commercial PET EVOO bottle and (**d**) 1 L commercial glass bottle, respectively, before and after blending with 20% SOY. (**e**) $\Delta C_{EVOO}/C_{EVOO}$ ($\pm\sigma$) (normalized by sensor area) vs. container type for EVOO blended with 20% SOY. Extra virgin olive oil−EVOO and soybean oil−SOY.

3.6. Automated EVOO Adulteration Detection System

The graphical user interface (GUI) of FDC2214EVM is limited by its re-programming capability, which prevents its implementation for developing fully automated systems for inline implementation and remote monitoring. Hence, for further development, the USB to I2C serial communication for data acquisition was performed using Arduino instead of the FDC2214 Sensing solutions GUI and the FDC2214 sensing module was re-designed in-house and fabricated in a foundry (JLCPCB, Shenzhen, China).

Figure 10a shows the Arduino-based sensing setup for automated detection of adulteration in EVOO. The in-house designed FDC2214 was interfaced with Arduino IDE via Arduino Pro Mini (3.3 V, 8 MHz, Sparkfun, Niwot, CO, USA). The Arduino Pro Mini was connected to a laptop via an FTDI basic (3.3 V, 8 MHz, Sparkfun, Niwot, CO, USA) breakout chip for USB to serial IC data transmission. The baud rate was set to 51,200 and the data acquisition rate was 100 ms. RealTerm serial terminal open-source software was used for the data logging process. A relative capacitance ($\Delta C_{EVOO}/C_{EVOO}$) threshold (>0.015%) was set in the Arduino code with a LED output showing two states for EVOO (OFF) and adulterated EVOO (ON), respectively. Kst real-time open-source dataset plotting tool was used

for live data visualization. The response of the in-house developed Arduino-based system is comparable to the FDC2214EVM as shown in Figure 10b, which confirms the consistency of the earlier observed trend and demonstrates the successful translation of the feasibility study to a preliminary prototype. This Arduino-based system offers several advantages in terms of cost, footprint and multiplexing summarized in Table 3. Figure 10c shows the photographs of the FDC2214EVM and the components of the in-house designed FDC2214 system. The newly developed system is 89% lower in cost and 32% smaller in footprint, compared to the FDC2214EVM-based system, respectively. Although the FDC2214 used in both systems have four channels, the Arduino-based system offers greater flexibility in terms of multiplexing for multi-channel monitoring, which could significantly boost the inspection throughput. Such an Arduino-based system further allows multi-channel cum multi-product monitoring as shown in Figure 10d. Four FDCs (FDC1, FDC2, FDC3 and FDC4) were multiplexed using one in-house designed TCA9548A, 1-to-8 I^2C multiplexer (Adafruit, New York, NY, USA) to generate 16 active channels. Channel 1 (CH1) of FDC1 and FDC2 were connected to two different (sensor area and inter-electrode gap) in-house designed sensor electrodes to monitor two separate non-polar liquids (honey and oil) packaged in different containers (size, shape and wall thickness) simultaneously. The different baselines and capacitance changes seen in the live plotting tool (Figure 10e) for the two liquids affirm the detection of different packaged liquid dielectrics. It is possible to operate up to 8 FDCs yielding 32 active channels using a single multiplexer, which is not possible in FDC2214EVM due to the limitations of the dedicated GUI. Herein, the components are designed separately and connected via wires to evaluate the proof of concept. Hence, further shrinking of the footprint and reduction in system cost is possible by integrating all individual components on a single PCB board for batch fabrication.

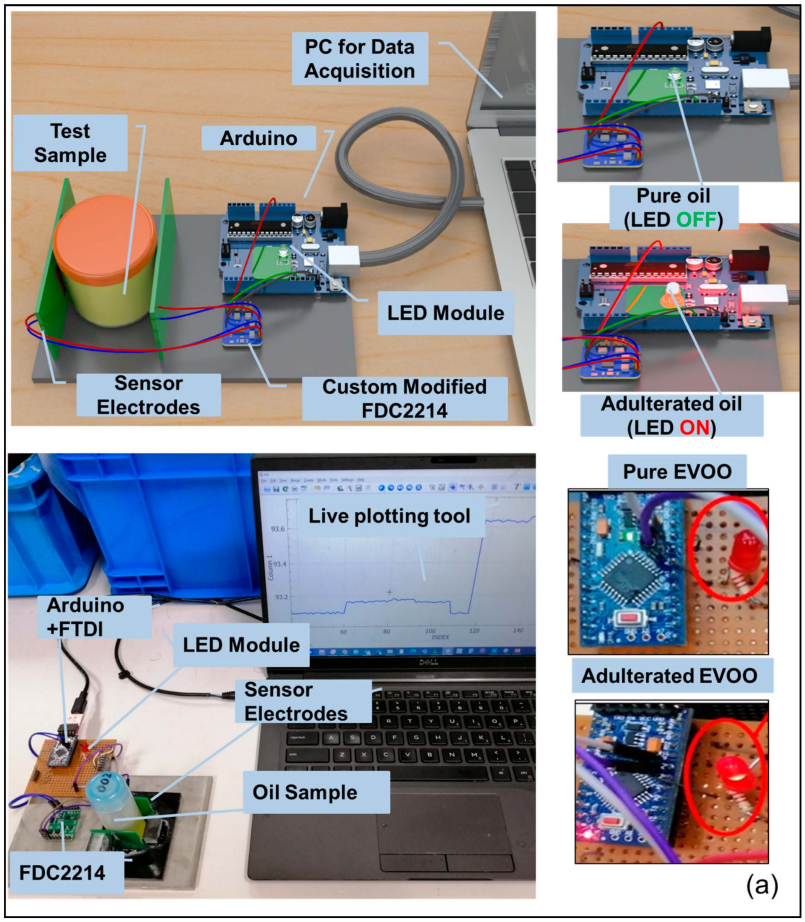


Figure 10. *Cont.*

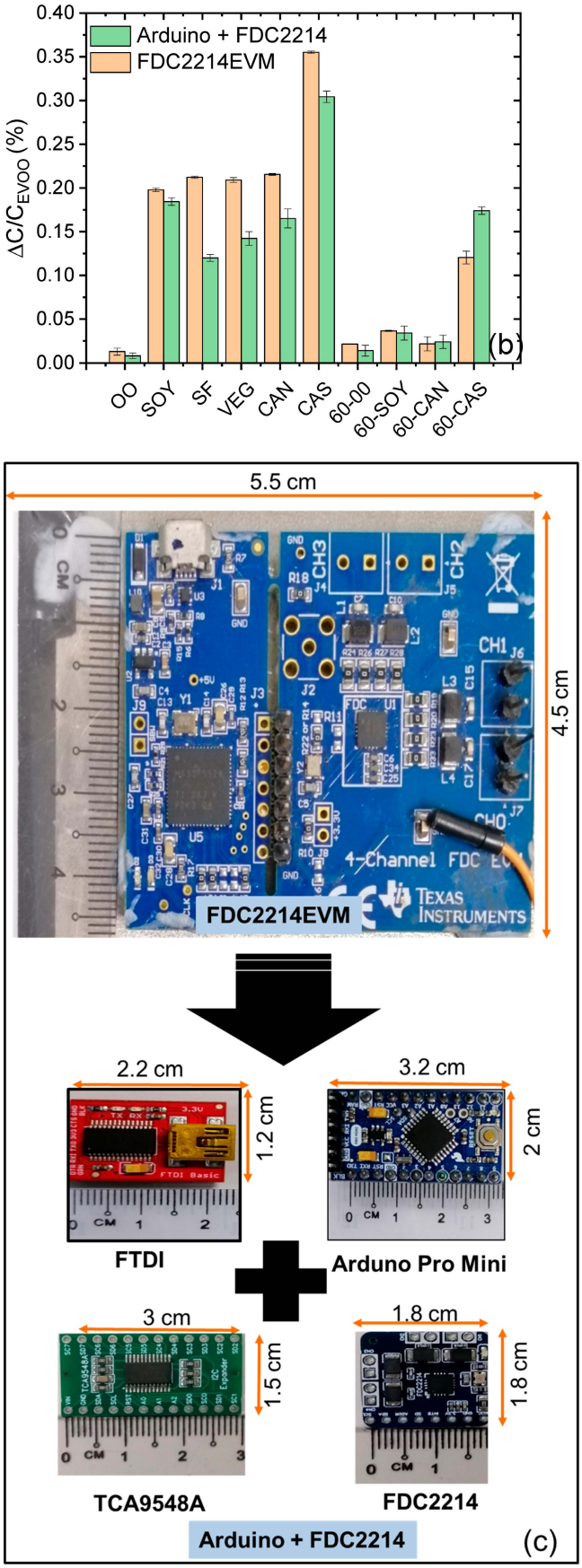


Figure 10. *Cont.*

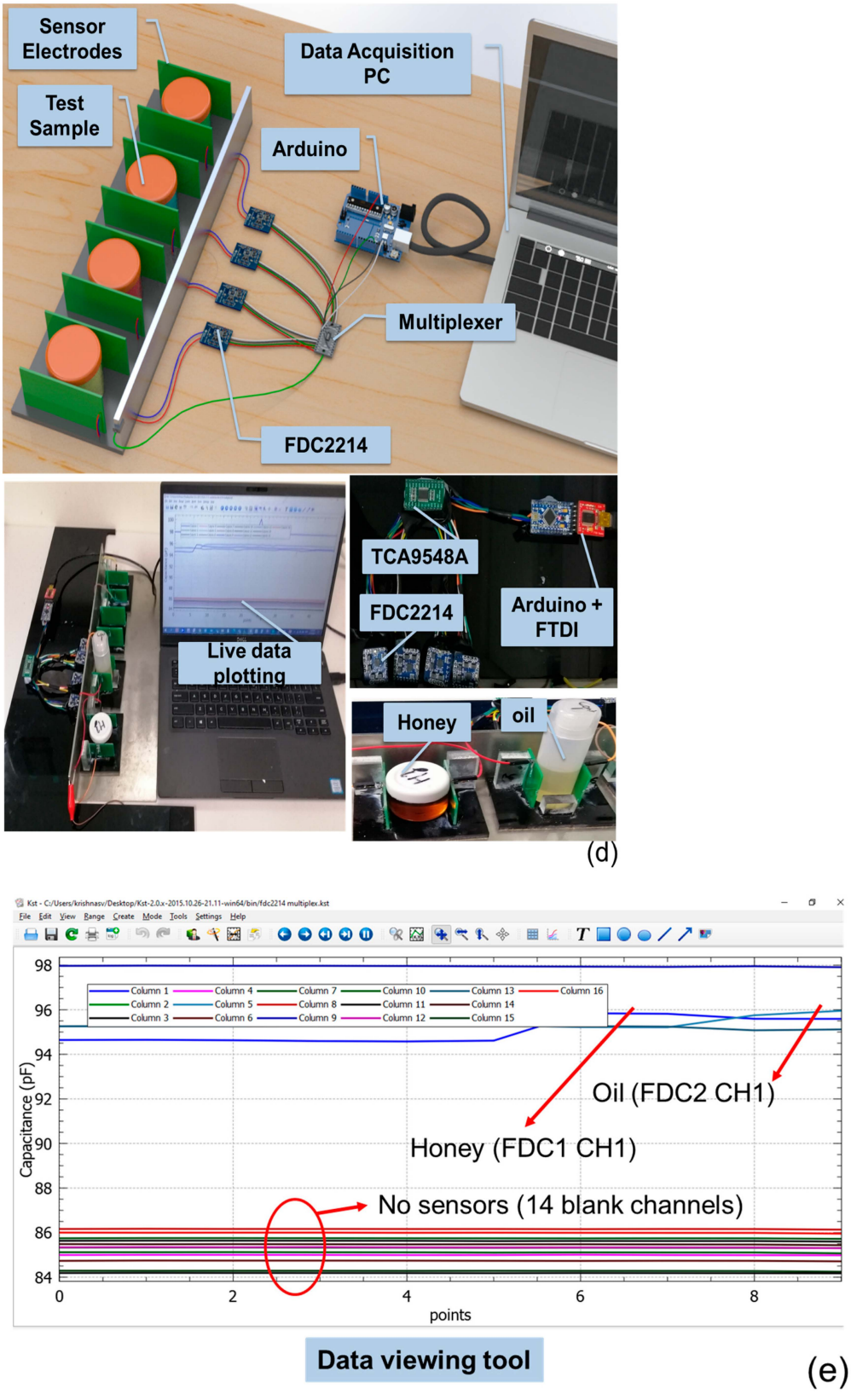


Figure 10. Automated low-cost capacitive EVOO adulteration detection system: (**a**) Arduino-based FDC2214 sensing set up with LED output showing EVOO (OFF) and adulterated EVOO (ON) detection through threshold setting. (**b**) Comparison of $\Delta C_{EVOO}/C_{EVOO}$ ($\pm\sigma$) of FDC2214EVM and Arduino-based EVOO adulteration testing system for adulterant oils and EVOO with 60%

adulteration. (**c**) Photographs of the footprint comparison of FDC2214EVM vs Arduino-based FDC2214 with corresponding in-house PCB design schematics. (**d**) General schematic of a multi-channel capacitive adulteration monitoring setup (**top**) and the photographs of the 16-channel operation with four FDC2214 breakout chips with enlarged views showing the sensor connections and liquids under test (**bottom**). (**e**) Real-time capacitance visualization of 16 live channels with two active channels (electrodes connected) for monitoring two different liquids (honey and oil) contained in different containers. Extra virgin olive oil−EVOO, olive oil−OO, soybean oil−SOY, sunflower oil−SF, vegetable oil−VEG, canola oil−CAN and castor oil−CAS.

Table 3. Comparison of FDC2214EVM and in-house designed FDC2214 with Arduino.

Criteria	FDC2214EVM	Arduino + FDC2214
Cost (USD)	510	54
Footprint (cm^2)	25	17
Multiplexing FDC (channels)	Not possible (4)	Yes (32)
Automated threshold detection	No	Yes

3.7. Comparison with Other Industrial Adulteration Detection Methods

Spectroscopy and chromatographic techniques are widely used industry standards for the authenticity check of edible oils [87]. Table 4 shows a comparison of the proposed capacitive system against the current industrial standards employed for oil adulteration detection. As expected, the detection limits of our proposed method are lower compared to traditional methods due to the presence of the container/packager barrier between the oil and the sensing surface. On the other hand, the existing industrial techniques, despite showing low detection limits, require sample extraction, specific sample volume, sample treatment/preparation, dedicated cuvettes and skilled operators to perform offline analysis ex situ, which significantly increases the screening time. Consequently, the number of samples inspected is reduced, which results in unnecessary batch rejection of samples based on the output of random sampling. The proposed system outperforms existing industrial methods in terms of cost, footprint and detection throughput while offering a novel non-destructive tool to aid quick screening for packaged products.

Table 4. A benchmark table of the proposed capacitive detection against the standard industrial edible oil authenticity testing methods.

Criteria	Spectroscopy	Chromatography	This Work
Response time	5 s–1.5 h	15 min–40 min	<1 s
Sample extraction	Yes	Yes	No
Throughput (samples/min)	<10	0	>60
Cost/system (USD)	1200–150,000	3000–15,000	50–500
Detection limit (%)	<1% [88–90]	<1% [91–93]	>10% (except for castor oil > 1%)
Footprint	Large	Very Large	Small
Deployability	Offline	Offline	Inline
Waste generation	Yes	Yes	No

4. Conclusions and Future Work

In summary, the proposed non-destructive capacitive detection scheme successfully classified good and adulterated oils non-invasively without requiring any sample extraction via through-package/container testing. The proposed method indirectly relies on the differences in dielectric properties of the oil from blending to make qualitative and quantitative assessment of oil capacitance deviations due to blending without complex requiring complex dielectric calculations and sophisticated instrumentation. The adulteration detection limit and sensitivity of the capacitance sensing system depend on the nature

(density, fatty acid content and dielectric constant) of the adulterant. The fast detection time and sensitivity achieved were achieved using simple electronic circuitry making it cheap and scalable for large-volume and high-speed production in FMCG lines. The non-invasive screening allows 100% inline package/container inspection for oil quality check, without the need to tamper with the container/package sealing for sample extraction thereby reducing wastage from batch re-jects. The major advantage of this quick screening method would be in situ quality control check, without overwhelming the few available laboratories with unnecessary requests. In other words, if the capacitive-based analysis gives a 'positive' result (i.e., adulterant might be present), then further specific analyses could be requested from dedicated laboratories for finding chemical composition; on the other hand, if the result is negative, then there is no need to carry out additional expensive and time-consuming analyses. This tool is not aimed at quantitative estimation of the chemical composition of EVOO fatty acids due to adulteration, or dielectric permittivity evaluation, instead, it focuses on providing a platform for rapid in situ qualitative screening, which is absent in current food industries.

Some of the limitations of the proposed system include its inability to perform authenticity checks through metallic containers (very few edible oils are packaged in metal jars) as the metallic body acts as the ground and drains the capacitive field. A possible solution to overcome this is to couple the capacitance electrodes with inductance to measure the impedance of the container with oil under test. Additionally, the applicability of the proposed method to edible oils in general needs evaluation on a case-by-case basis considering the vast range of adulterants and variations in oils due to pre- and post-harvest factors.

The current work involves in-house PCB design of a fully integrated capacitance board with all the components (electrodes, Arduino, FDC2214 and multiplexer) assembled on board to further reduce the cost and footprint. The future work would involve the software and hardware design for automation of a standalone capacitance-based adulteration testing prototype system with a pass/fail criterion suitable for analysing moving packaged containers with different edible liquids (e.g., honey, milk, etc.).

Supplementary Materials: The following supporting information can be downloaded at: https://www.mdpi.com/article/10.3390/electronics12020359/s1, Supplementary data associated with this article can be found in supporting information.

Author Contributions: Conceptualization, H.K.S.V.M.; methodology, H.K.S.V.M.; software, C.F.N. and P.P.A.; data curation, H.K.S.V.M. and C.F.N.; formal analysis, H.K.S.V.M. and C.F.N.; investigation, H.K.S.V.M.; P.P.A. and C.F.N.; funding acquisition, A.A.M. and Z.Z.W.; project administration, Z.Z.W. and A.A.M.; resources, Z.Z.W. and A.A.M.; supervision, Z.Z.W. and A.A.M.; validation, H.K.S.V.M. and Z.Z.W.; visualization, H.K.S.V.M.; writing—original draft, H.K.S.V.M.; writing—review and editing, Z.Z.W. and A.A.M. All authors have read and agreed to the published version of the manuscript.

Funding: This research/project is supported by financial assistance from the Advanced Remanufacturing and Technology Centre (ARTC)—a research institute under the Agency for Science, Technology and Research (A*STAR), Singapore.

Data Availability Statement: Data is unavailable as the raw/processed data required to reproduce the above findings cannot be shared at this time as the data also forms part of an ongoing study.

Conflicts of Interest: The authors declare no conflict of interest.

References

1. Bansal, S.; Singh, A.; Mangal, M.; Mangal, A.K.; Kumar, S. Food Adulteration: Sources, Health Risks, and Detection Methods. *Crit. Rev. Food Sci. Nutr.* **2017**, *57*, 1174–1189. [CrossRef] [PubMed]
2. Jimenez-Lopez, C.; Carpena, M.; Lourenço-Lopes, C.; Gallardo-Gomez, M.; Lorenzo, J.M.; Barba, F.J.; Prieto, M.A.; Simal-Gandara, J. Bioactive Compounds and Quality of Extra Virgin Olive Oil. *Foods* **2020**, *9*, 1014. [CrossRef] [PubMed]
3. Global Olive Oil Consumption at Record High in 2020. Available online: https://ambrosiamagazine.com/global-olive-oil-consumption-at-record-high-in-2020/ (accessed on 17 December 2022).

4. Levi, R.; Singhvi, S.; Zheng, Y. Economically Motivated Adulteration in Farming Supply Chains. *Manag. Sci.* **2020**, *66*, 209–226. [CrossRef]
5. Moore, J.C.; Spink, J.; Lipp, M. Development and Application of a Database of Food Ingredient Fraud and Economically Motivated Adulteration from 1980 to 2010. *J. Food Sci.* **2012**, *77*, R118–R126. [CrossRef] [PubMed]
6. Tay, A.; Singh, R.K.; Krishnan, S.S.; Gore, J.P. Authentication of Olive Oil Adulterated with Vegetable Oils Using Fourier Transform Infrared Spectroscopy. *Lebenson. Wiss. Technol.* **2002**, *35*, 99–103. [CrossRef]
7. Ollivier, D.; Artaud, J.; Pinatel, C.; Durbec, J.P.; Guérère, M. Triacylglycerol and Fatty Acid Compositions of French Virgin Olive Oils. Characterization by Chemometrics. *J. Agric. Food Chem.* **2003**, *51*, 5723–5731. [CrossRef]
8. Giuffrè, A.M. The Effects of Cultivar and Harvest Year on the Fatty Alcohol Composition of Olive Oils from Southwest Calabria (Italy). *Grasas Aceites* **2014**, *65*, e011. [CrossRef]
9. Giuffrè, A.M.; Louadj, L. Influence of Crop Season and Cultivar on Sterol Composition of Monovarietal Olive Oils in Reggio Calabria (Italy). *Czech J. Food Sci.* **2013**, *31*, 256–263. [CrossRef]
10. Skiada, V.; Agriopoulou, S.; Tsarouhas, P.; Katsaris, P.; Stamatelopoulou, E.; Varzakas, T. Evaluation and Origin Discrimination of Two Monocultivar Extra Virgin Olive Oils, Cultivated in the Coastline Part of North-Western Greece. *Appl. Sci.* **2020**, *10*, 6733. [CrossRef]
11. Giuffrè, A.M. Wax Ester Variation in Olive Oils Produced in Calabria (Southern Italy) during Olive Ripening. *J. Am. Oil Chem. Soc.* **2014**, *91*, 1355–1366. [CrossRef]
12. Franco, M.N.; Galeano-Díaz, T.; Sánchez, J.; De Miguel, C.; Martín-Vertedor, D. Total Phenolic Compounds and Tocopherols Profiles of Seven Olive Oil Varieties Grown in the South-West of Spain. *J. Oleo Sci.* **2014**, *63*, 115–125. [CrossRef]
13. Giuffrè, A.M.; Caracciolo, M.; Zappia, C.; Capocasale, M.; Poiana, M. Effect of Heating on Chemical Parameters of Extra Virgin Olive Oil, Pomace Olive Oil, Soybean Oil and Palm Oil. *Ital. J. Food Sci.* **2018**, *30*, 715–739. [CrossRef]
14. Pedan, V.; Popp, M.; Rohn, S.; Nyfeler, M.; Bongartz, A. Characterization of Phenolic Compounds and Their Contribution to Sensory Properties of Olive Oil. *Molecules* **2019**, *24*, 2041. [CrossRef]
15. Gouvinhas, I.; Machado, J.; Gomes, S.; Lopes, J.; Martins-Lopes, P.; Barros, A.I.R.N.A. Phenolic Composition and Antioxidant Activity of Monovarietal and Commercial Portuguese Olive Oils. *J. Am. Oil Chem. Soc.* **2014**, *91*, 1197–1203. [CrossRef]
16. Lazzerini, C.; Domenici, V. Pigments in Extra-Virgin Olive Oils Produced in Tuscany (Italy) in Different Years. *Foods* **2017**, *6*, 25. [CrossRef]
17. Gandul-Rojas, B.; Cepero, M.R.-L.; Mínguez-Mosquera, M.I. Use of Chlorophyll and Carotenoid Pigment Composition to Determine Authenticity of Virgin Olive Oil. *J. Am. Oil Chem. Soc.* **2000**, *77*, 853–858. [CrossRef]
18. Giuffrè, A.M. The Effect of Cultivar and Harvest Season on the N-Alkane and the n-Alkene Composition of Virgin Olive Oil. *Eur. Food Res. Technol.* **2021**, *247*, 25–36. [CrossRef]
19. Giuffrè, A.M.; Capocasale, M.; Macrì, R.; Caracciolo, M.; Zappia, C.; Poiana, M. Volatile Profiles of Extra Virgin Olive Oil, Olive Pomace Oil, Soybean Oil and Palm Oil in Different Heating Conditions. *Lebenson. Wiss. Technol.* **2020**, *117*, 108631. [CrossRef]
20. Visioli, F.; Bellomo, G.; Galli, C. Free Radical-Scavenging Properties of Olive Oil olyphenols. *Biochem. Biophys. Res. Commun.* **1998**, *247*, 60–64. [CrossRef]
21. Pérez-Jiménez, F.; López-Miranda, J.; Mata, P. Protective Effect of Dietary Monounsaturated Fat on Arteriosclerosis: Beyond Cholesterol. *Atherosclerosis* **2002**, *163*, 385–398. [CrossRef]
22. Yaqoob, P.; Knapper, J.A.; Webb, D.H.; Williams, C.M.; Newsholme, E.A.; Calder, P.C. Effect of Olive Oil on Immune Function in Middle-Aged Men. *Am. J. Clin. Nutr.* **1998**, *67*, 129–135. [CrossRef] [PubMed]
23. Yago, M.D.; Martinez-Victoria, E.; Mañas, M.; Martinez, M.A.; Mataix, J. Plasma Peptide YY and Pancreatic Polypeptide in Dogs after Long-Term Adaptation to Dietary Fats of Different Degrees of Saturation: Olive and Sunflower Oil. *J. Nutr. Biochem.* **1997**, *8*, 502–507. [CrossRef]
24. Assy, N.; Nassar, F.; Nasser, G.; Grosovski, M. Olive Oil Consumption and Non-Alcoholic Fatty Liver Disease. *World J. Gastroenterol.* **2009**, *15*, 1809–1815. [CrossRef] [PubMed]
25. Rouas, S.; Rahmani, M.; El Antari, A.; Idrissi, D.J.; Souizi, A.; Maata, N. Effect of geographical conditions (altitude and pedology) and age of olive plantations on the typicality of olive oil in Moulay Driss Zarhoun. *Mediterr. J. Biol.* **2016**, *1*, 128–137.
26. Tupper, N. Spanish Olive Oil under Constant Threat from Climate Change. Available online: https://www.oliveoiltimes.com/world/spanish-olive-oil-under-constant-threat-from-climate-change/29618 (accessed on 16 December 2022).
27. Rached, M.B.; Galaverna, G.; Cirlini, M.; Boujneh, D.; Zarrouk, M.; Guerfel, M. Pedologic Factors Affecting Virgin Olive Oil Quality of "Chemlali" Olive Trees (*Olea europaea* L.). *J. Oleo Sci.* **2017**, *66*, 907–915. [CrossRef] [PubMed]
28. Romero, N.; Saavedra, J.; Tapia, F.; Sepúlveda, B.; Aparicio, R. Influence of Agroclimatic Parameters on Phenolic and Volatile Compounds of Chilean Virgin Olive Oils and Characterization Based on Geographical Origin, Cultivar and Ripening Stage: Effect of Agroclimatic Parameters on Compounds Responsible for the Flavor of EVOO. *J. Sci. Food Agric.* **2016**, *96*, 583–592. [CrossRef]
29. Golbach, H.E. A critical review on current hypothesis concerning the role of boron in higher plants: Suggestions for further research and methodological requirements. *J. Trace Microprobe Tech.* **1997**, *15*, 51–91.
30. Gutiérrez, F.; Jímenez, B.; Ruíz, A.; Albi, M.A. Effect of Olive Ripeness on the Oxidative Stability of Virgin Olive Oil Extracted from the Varieties Picual and Hojiblanca and on the Different Components Involved. *J. Agric. Food Chem.* **1999**, *47*, 121–127. [CrossRef]

31. Méndez, A.I.; Falqué, E. Effect of Storage Time and Container Type on the Quality of Extra-Virgin Olive Oil. *Food Control* **2007**, *18*, 521–529. [CrossRef]
32. Di Giovacchino, L.; Sestili, S.; Di Vincenzo, D. Influence of olive processing on virgin olive oil quality. *Eur. J. Lipid Sci. Technol.* **2002**, *104*, 587–601. [CrossRef]
33. Gharbi, I.; Issaoui, M.; Mehri, S.; Cheraief, I.; Sifi, S.; Hammami, M. Agronomic and Technological Factors Affecting Tunisian Olive Oil Quality. *Agric. Sci.* **2015**, *6*, 513–526. [CrossRef]
34. Gargouri, B.; Zribi, A.; Bouaziz, M. Effect of Containers on the Quality of Chemlali Olive Oil during Storage. *J. Food Sci. Technol.* **2015**, *52*, 1948–1959. [CrossRef]
35. Available online: https://eur-lex.europa.eu/legal-content/EN/TXT/PDF/?uri=CELEX:01991R2568-20161204&from=IT (accessed on 16 December 2022).
36. Olive Oil. Available online: https://www.internationaloliveoil.org/olive-world/olive-oil/ (accessed on 16 December 2022).
37. SECTION 2. Codex Standards for Fats and Oils from Vegetable Sources. Available online: https://www.fao.org/3/y2774e/y2774e04.htm (accessed on 17 December 2022).
38. Li, B.; Wang, H.; Zhao, Q.; Ouyang, J.; Wu, Y. Rapid Detection of Authenticity and Adulteration of Walnut Oil by FTIR and Fluorescence Spectroscopy: A Comparative Study. *Food Chem.* **2015**, *181*, 25–30. [CrossRef]
39. Azizian, H.; Mossoba, M.M.; Fardin-Kia, A.R.; Delmonte, P.; Karunathilaka, S.R.; Kramer, J.K.G. Novel, Rapid Identification, and Quantification of Adulterants in Extra Virgin Olive Oil Using near-Infrared Spectroscopy and Chemometrics. *Lipids* **2015**, *50*, 705–718. [CrossRef]
40. Duraipandian, S.; Petersen, J.C.; Lassen, M. Authenticity and Concentration Analysis of Extra Virgin Olive Oil Using Spontaneous Raman Spectroscopy and Multivariate Data Analysis. *Appl. Sci.* **2019**, *9*, 2433. [CrossRef]
41. Fragaki, G.; Spyros, A.; Siragakis, G.; Salivaras, E.; Dais, P. Detection of Extra Virgin Olive Oil Adulteration with Lampante Olive Oil and Refined Olive Oil Using Nuclear Magnetic Resonance Spectroscopy and Multivariate Statistical Analysis. *J. Agric. Food Chem.* **2005**, *53*, 2810–2816. [CrossRef]
42. Carranco, N.; Farrés-Cebrián, M.; Saurina, J.; Núñez, O. Authentication and Quantitation of Fraud in Extra Virgin Olive Oils Based on HPLC-UV Fingerprinting and Multivariate Calibration. *Foods* **2018**, *7*, 44. [CrossRef]
43. Drira, M.; Guclu, G.; Portolés, T.; Jabeur, H.; Kelebek, H.; Selli, S.; Bouaziz, M. Safe and Fast Fingerprint Aroma Detection in Adulterated Extra Virgin Olive Oil Using Gas Chromatography–Olfactometry-Mass Spectrometry Combined with Chemometrics. *Food Anal. Methods* **2021**, *14*, 2121–2135. [CrossRef]
44. Meenu, M.; Cai, Q.; Xu, B. A Critical Review on Analytical Techniques to Detect Adulteration of Extra Virgin Olive Oil. *Trends Food Sci. Technol.* **2019**, *91*, 391–408. [CrossRef]
45. Lizhi, H.; Toyoda, K.; Ihara, I. Dielectric Properties of Edible Oils and Fatty Acids as a Function of Frequency, Temperature, Moisture and Composition. *J. Food Eng.* **2008**, *88*, 151–158. [CrossRef]
46. Bumbrah, G.S.; Sharma, R.M. Raman Spectroscopy—Basic Principle, Instrumentation and Selected Applications for the Characterization of Drugs of Abuse. *Egypt. J. Forensic Sci.* **2016**, *6*, 209–215. [CrossRef]
47. Raveendran, S.; Parameswaran, B.; Ashok, P. Microbial Poly-3-Hydroxybutyrate and Related Copolymers. In *Industrial Biorefineries & White Biotechnology*; Elsevier: Amsterdam, The Netherlands, 2015; pp. 575–605, ISBN 9780444634535.
48. Yang, H.; Irudayaraj, J.; Paradkar, M. Discriminant Analysis of Edible Oils and Fats by FTIR, FT-NIR and FT-Raman Spectroscopy. *Food Chem.* **2005**, *93*, 25–32. [CrossRef]
49. Hamdan, K.; Abd Aziz, S.; Yahya, A.; Rokhani, F.Z.; Steward, B.L. Detection of Sludge Contamination in Crude Palm Oil Using Dielectric Spectroscopy. *Trans. ASABE* **2015**, *58*, 227–232. [CrossRef]
50. Bakhshiani, M.; Suster, M.A.; Mohseni, P. A 9 MHz-2.4 GHz Fully Integrated Transceiver IC for a Microfluidic-CMOS Platform Dedicated to Miniaturized Dielectric Spectroscopy. *IEEE Trans. Biomed. Circuits Syst.* **2015**, *9*, 849–861. [CrossRef] [PubMed]
51. Maji, D.; Suster, M.A.; Stavrou, E.; Gurkan, U.A.; Mohseni, P. Monitoring Time Course of Human Whole Blood Coagulation Using a Microfluidic Dielectric Sensor with a 3D Capacitive Structure. In Proceedings of the 2015 37th Annual International Conference of the IEEE Engineering in Medicine and Biology Society (EMBC), Milan, Italy, 25–29 August 2015; pp. 5904–5907. [CrossRef]
52. Waygood, A. *An Introduction to Electrical Science*; Routledge: Oxford, UK, 2013; ISBN 9781135071141.
53. Warsito, W.; Marashdeh, Q.; Fan, L.-S. Electrical Capacitance Volume Tomography. *IEEE Sens. J.* **2007**, *7*, 525–535. [CrossRef]
54. Eren, H.; Goh, J. Capacitance and capacitance measurements. In *Electrical Measurement, Signal Processing, and Displays*; Webster, J.G., Ed.; CRC Press: Boca Raton, FL, USA, 2003; ISBN 9780429214417. [CrossRef]
55. Hu, X.; Yang, W. Planar Capacitive Sensors—Designs and Applications. *Sens. Rev.* **2010**, *30*, 24–39. [CrossRef]
56. Baxter, L.K. *Capacitive Sensors: Design and Applications*; John Wiley & Sons: Nashville, TN, USA, 1996; ISBN 9780780353510.
57. Pérez Sanjurjo, J.; Prefasi, E.; Buffa, C.; Gaggl, R. A Capacitance-to-Digital Converter for MEMS Sensors for Smart Applications. *Sensors* **2017**, *17*, 1312. [CrossRef]
58. Nelson, S.O.; Trabelsi, S. Historical Development of Grain Moisture Measurement and Other Food Quality Sensing through Electrical Properties. *IEEE Instrum. Meas. Mag.* **2016**, *19*, 16–23. [CrossRef]
59. Sanaeifar, A.; Jafari, A.; Golmakani, M.-T. Fusion of Dielectric Spectroscopy and Computer Vision for Quality Characterization of Olive Oil during Storage. *Comput. Electron. Agric.* **2018**, *145*, 142–152. [CrossRef]
60. Soltani, M.; Alimardani, R.; Omid, M. Evaluating Banana Ripening Status from Measuring Dielectric Properties. *J. Food Eng.* **2011**, *105*, 625–631. [CrossRef]

61. Sacilik, K.; Tarimci, C.; Colak, A. Moisture Content and Bulk Density Dependence of Dielectric Properties of Safflower Seed in the Radio Frequency Range. *J. Food Eng.* **2007**, *78*, 1111–1116. [CrossRef]
62. Wang, B.; Pan, P.; McDonald, T.P.; Wang, Y. Development of a Capacitance Sensing System for Monitoring Moisture Content of Spray Dried Gelatin Powders. *J. Food Eng.* **2017**, *195*, 247–254. [CrossRef]
63. Rashvand, M.; Omid, M.; Mobli, H.; Firouz, M.S. Adulteration Detection in Olive Oil Using Dielectric Technique and Data Mining. Sens. *BioSens. Res.* **2016**, *11*, 33–36. [CrossRef]
64. Lizhi, H.; Toyoda, K.; Ihara, I. Discrimination of Olive Oil Adulterated with Vegetable Oils Using Dielectric Spectroscopy. *J. Food Eng.* **2010**, *96*, 167–171. [CrossRef]
65. Salila Vijayalal Mohan, H.K.; Alexander Malcolm, A.; Cheng, F. Low-Cost Contactless Monitoring of Aseptic Package Integrity and Content Quality Using Capacitance. *Food Packag. Shelf Life* **2020**, *26*, 100598. [CrossRef]
66. Salila Vijayalal Mohan, H.K.; Toh, C.H.; Malcolm, A.A. A Novel Low-Cost Contactless Capacitive Evaluation Approach for Capping Integrity Assessment of Food and Beverage Containers. *Sens. Actuators Rep.* **2022**, *4*, 100088. [CrossRef]
67. Pan, J.; Li, Y.; Luo, Y.; Zhang, X.; Yang, Z.; Tai Wong, D.L.; Niu, X.; Tham, C.-K.; Thean, A.V.-Y. Seal Integrity Testing Utilizing Non-Destructive Capacitive Sensing for Product Packaging Assurance. In Proceedings of the 2020 IEEE SENSORS, Rotterdam, The Netherlands, 25–28 October 2020.
68. Salila Vijayalal Mohan, H.K.; Aaron, T.V.Y.; Nayak, S. Method and System for Integrity Testing of Sachets. World Patent 20210372961:A1, 31 October 2019. Available online: https://patentscope.wipo.int/search/en/detail.jsf?docId=WO2019209180 (accessed on 16 November 2022).
69. Wang, D. FDC1004: Basics of Capacitive Sensing and Applications. Available online: https://www.ti.com/lit/pdf/snoa927 (accessed on 17 December 2022).
70. Salila Vijayalal Mohan, H.K.; An, J.; Liao, K.; Wong, C.H.; Zheng, L. Detection and Classification of Host–Guest Interactions Using β-Cyclodextrin-Decorated Carbon Nanotube-Based Chemiresistors. *Curr. Appl. Phys.* **2014**, *14*, 1649–1658. [CrossRef]
71. Salila Vijayalal Mohan, H.K.; Chee, W.K.; Li, Y.; Nayak, S.; Poh, C.L.; Thean, A.V.Y. A Highly Sensitive Graphene Oxide Based Label-Free Capacitive Aptasensor for Vanillin Detection. *Mater. Des.* **2020**, *186*, 108208. [CrossRef]
72. Liao, S.; Dourmashkin, P.A.; Belcher, J. *Chapter 5 Capacitance and Dielectrics*; MIT: Cambridge, MA, USA, 2004; pp. 1–46. Available online: http://web.mit.edu/viz/EM/visualizations/notes/index.htm (accessed on 10 January 2023).
73. Gillis, K.D. Capacitance Measurement. In *Encyclopedia of Neuroscience*; Springer: Berlin/Heidelberg, Germany, 2008; pp. 560–563, ISBN 9783540237358.
74. Ragni, L.; Iaccheri, E.; Cevoli, C.; Berardinelli, A.; Bendini, A.; Toschi, T.G. A Capacitive Technique to Assess Water Content in Extra Virgin Olive Oils. *J. Food Eng.* **2013**, *116*, 246–252. [CrossRef]
75. Aparicio, R.; Harwood, J. (Eds.) *Handbook of Olive Oil*; Springer: Boston, MA, USA, 2013; ISBN 9781461477761.
76. Sagiroglu, A.; Isbilir, S.Ş.; Ozcan, M.H.; Paluzar, H.; Toprakkiran, N.M. Comparison of Biodiesel Productivities of Different Vegetable Oils by Acidic Catalysis. *Chem. Ind. Chem. Eng. Q.* **2011**, *17*, 53–58. [CrossRef]
77. Kostik, V.; Memeti, S.; Bauer, B. Fatty Acid Composition of Edible Oils and Fats. *J. Hyg. Eng. Des.* **2013**, *4*, 112–116.
78. Artavia, G.; Granados-Chinchilla, F. Discrimination, Quantitation, and Identification of Edible Vegetable Oil Blends Based on Their Fatty Acid Profiles. *Akad. Gıda* **2021**, *19*, 244–256. [CrossRef]
79. Gunstone, F.D. Production and Trade of Vegetable Oils. In *Vegetable Oils in Food Technology*; Wiley-Blackwell: Oxford, UK, 2011; pp. 1–24, ISBN 9781444339925.
80. Zeng, Q.; Dong, G. Influence of Load and Sliding Speed on Super-Low Friction of Nitinol 60 Alloy under Castor Oil Lubrication. *Tribol. Lett.* **2013**, *52*, 47–55. [CrossRef]
81. De Carvalho, L.M.; Abreu, W.C.D.; Silva, M.D.G.D.O.; Lima, J.R.D.O.; Oliveira, J.E.D.; Matos, J.M.E.D.; de Moura, C.V.; Moura, E.M.D. Heterogeneous Catalysis Afford Biodiesel of Babassu, Castor Oil and Blends. *J. Braz. Chem. Soc.* **2013**, *24*, 550–557. [CrossRef]
82. Ghosh, S.; Holmes, M.; Povey, M. Temperature Dependence of Bulk Viscosity in Edible Oils Using Acoustic Spectroscopy. *J. Food Process. Technol.* **2017**, *8*, 2. [CrossRef]
83. Siddique, B.M.; Ahmad, A.; Ibrahim, M.H.; Hena, S.; Rafatullah, M. Physico-Chemical Properties of Blends of Palm Olein with Other Vegetable Oils. *Grasas Aceites* **2010**, *61*, 423–429. [CrossRef]
84. Karuppuswami, S.; Kaur, A.; Arangali, H.; Chahal, P.P. A Hybrid Magnetoelastic Wireless Sensor for Detection of Food Adulteration. *IEEE Sens. J.* **2017**, *17*, 1706–1714. [CrossRef]
85. Amat Sairin, M.; Abd Aziz, S.; Yoke Mun, C.; Khaled, A.Y.; Rokhani, F.Z. Analysis and Prediction of the Major Fatty Acids in Vegetable Oils Using Dielectric Spectroscopy at 5–30 MHz. *PLoS ONE* **2022**, *17*, e0268827. [CrossRef]
86. Pecovska Gjorgjevich, M.; Andonovski, A.; Velevska, J. Dielectric Constant and Induced Dipole Moment of Edible Oils Subjected to Conventional Heating. *Maced. J. Chem. Chem. Eng.* **2012**, *31*, 285. [CrossRef]
87. Zhang, J.; Sun, H.; Lu, W. Recent Advances in Analytical Detection of Olive Oil Adulteration. *ACS Food Sci. Technol.* **2022**, *2*, 415–424. [CrossRef]
88. Borghi, F.T.; Santos, P.C.; Santos, F.D.; Nascimento, M.H.C.; Corrêa, T.; Cesconetto, M.; Pires, A.A.; Ribeiro, A.V.F.N.; Lacerda, V., Jr.; Romão, W.; et al. Quantification and Classification of Vegetable Oils in Extra Virgin Olive Oil Samples Using a Portable Near-Infrared Spectrometer Associated with Chemometrics. *Microchem. J.* **2020**, *159*, 105544. [CrossRef]

89. Jiménez-Carvelo, A.M.; Osorio, M.T.; Koidis, A.; González-Casado, A.; Cuadros-Rodríguez, L. Chemometric Classification and Quantification of Olive Oil in Blends with Any Edible Vegetable Oils Using FTIR-ATR and Raman Spectroscopy. *Lebenson. Wiss. Technol.* **2017**, *86*, 174–184. [CrossRef]
90. Jabeur, H.; Zribi, A.; Bouaziz, M. Extra-Virgin Olive Oil and Cheap Vegetable Oils: Distinction and Detection of Adulteration as Determined by GC and Chemometrics. *Food Anal. Methods* **2016**, *9*, 712–723. [CrossRef]
91. Yang, Y.; Ferro, M.D.; Cavaco, I.; Liang, Y. Detection and Identification of Extra Virgin Olive Oil Adulteration by GC-MS Combined with Chemometrics. *J. Agric. Food Chem.* **2013**, *61*, 3693–3702. [CrossRef]
92. Hajimahmoodi, M.; Vanderheyden, Y.; Sadeghi, N.; Jannat, B.; Oveisi, M.; Shahbazian, S. Gas-Chromatographic Fatty-Acid Fingerprints and Partial Least Squares Modeling as a Basis for the Simultaneous Determination of Edible Oil Mixtures. *Talanta* **2005**, *66*, 1108–1116. [CrossRef]
93. Luo, Y.; Gao, B.; Zhang, Y.; Yu, L.L. Detection of Olive Oil Adulteration with Vegetable Oils by Ultra-Performance Convergence Chromatography-Quadrupole Time-of-Flight Mass Spectrometry (UPC2-QTOF MS) Coupled with Multivariate Data Analysis Based on the Differences of Triacylglycerol Compositions. *Food Sci. Nutr.* **2020**, *8*, 3759–3767. [CrossRef]

Disclaimer/Publisher's Note: The statements, opinions and data contained in all publications are solely those of the individual author(s) and contributor(s) and not of MDPI and/or the editor(s). MDPI and/or the editor(s) disclaim responsibility for any injury to people or property resulting from any ideas, methods, instructions or products referred to in the content.